Chapter 1
Homogeneous Sliding Modes in Noisy Environments

published in "Emerging Trends in Sliding Mode Control Theory and Application", Studies in Systems, Decision and Control, Vol. 318, pp 1–46, Springer 2021

Avi Hanan, Adam Jbara and Arie Levant

Abstract. One of the main achievements of the High-Order Sliding-Mode Control (HOSMC) theory is the standardized output-feedback regulation based on the robust high-order differentiation. The method employs universal HOSM controllers valid for any relative degree combined with standard HOSM differentiators. In this chapter we present recently developed new universal controllers and filtering differentiators and demonstrate their output-feedback application in the presence of large sampling noises.

1.1 Introduction

Sliding mode (SM) control (SMC) [27, 53, 75, 78] has been introduced to effectively control uncertain processes. The method assumes choosing a proper system output σ called sliding variable to keep it at zero. The constraint $\sigma \equiv 0$ is to provide for the desired system performance and is established in finite time by a high-frequency switching control.

The control switching is inevitable due to the uncertainty of the system. Unfortunately, it produces undesired system vibrations called the chattering effect [9, 15, 34, 77].

While keeping the switching, the SM control itself can be done continuous. Its discontinuity can be shifted to the higher total derivatives of the sliding variable. The number r of the first discontinuous total time derivative $\sigma^{(r)}$ is called the SM order [44, 46]. The conventional SMs [27, 77] feature the first SM order. Higher-order SMs (HOSMs) are capable of successful chattering mitigation [10, 11, 16, 44], but are not able to completely remove it [15, 49]. Moreover, in fact the chattering can be considered as an inherent feature of sampling-based systems [49].

The output regulation is the most straightforward application of SMC due to the simplicity of choosing the tracking error as the sliding variable. A great number of papers employs this technique, here we only cite a few: [11, 19, 23, 24, 25, 26, 30, 33, 36, 39, 43, 46, 56, 63, 65, 67, 68, 74, 76]. SM-based differentiators [46, 45] are included in the feedback to produce finite-time (FT) exact derivatives of the sliding variable [2, 4, 7, 8, 22, 20, 29, 32, 42, 53, 66, 73].

Most above results are based on the application of the general homogeneity approach [6, 14, 41] to the SMC theory [12, 13, 35, 47, 54, 57, 65, 72, 69].

Till recently the invention of new SM controllers has been considered a difficult task [24, 46, 48], but recently numerous new controllers have been proposed together with general construction approaches [19][18][65][70][71]. Recent control template approaches [51, 38] belong to this category, and present very easy control design.

Standard SM-based differentiators [46] have been recently used to construct new filtering differentiators [59, 61]. These new differentiators combine their exactness and asymptotically optimal accuracy in the presence of noises [60] with the new strong noise filtering capabilities. In particular, they are capable of suppressing *unbounded* noises, provided some high-order local multiple integral of the noise is uniformly small. New hybrid differentiators [58, 7] feature the bilimit homogeneity [1]. They can be considered as hybrids of the linear filters [5] (high-gain observers) with the SM-based differentiators [46]. Such differentiators do not employ high gains, allow variable gains and feature fast FT convergence. Recently we have proposed equipping hybrid differentiators with the filtering capabilities [37].

In this chapter we demonstrate the implementation of new SM control templates [51, 38] in the output-feedback HOSM control and its new filtering capabilities in the presence of very large noises due to the filtering [59] and hybrid filtering [37] differentiators.

Notation. Let $\lfloor \cdot \rceil^m = |\cdot|^m \operatorname{sign}(\cdot)$ for any $m \geq 0$. Note that $\frac{\partial}{\partial x}|x|^{m+1} = (m+1)\lfloor x \rceil^m$ and $\frac{\partial}{\partial x}\lfloor x \rceil^{m+1} = (m+1)|x|^m$. A function of a set is the set of function values on this set. The norm $||x||$ stays for the standard Euclidean norm of x, $B_\varepsilon = \{x| \ ||x|| \leq \varepsilon\}$ and $||x||_h$ is a homogeneous norm. Let $a \diamond b$ be a binary operation for $a \in A, b \in B$, then $A \diamond B = \{a \diamond b | a \in A, b \in B\}$.

Depending on the context, we use the same notation $\vec{\xi}_k$ for both $(\xi, \dot{\xi}, ..., \xi^{(k)})$ and $(\xi_0, \xi_1, ..., \xi_k)$. We define the finite difference operator $\delta_j A = A(t_{j+1}) - A(t_j)$ for any sampled function $A(t_j)$.

1.2 Preliminaries

In this section we recall some basic homogeneity and stability notions.

1.2.1 Stability of differential inclusions

Let $T\mathbb{R}^{n_x}$ denote the tangent space to $\mathbb{R}^{n_x}$, and $T_x\mathbb{R}^{n_x}$ be the tangent space at the point $x \in \mathbb{R}^{n_x}$. Consider the differential inclusion (DI)

$$\dot{x} \in F(x),\ x \in \mathbb{R}^{n_x}, F(x) \subset T_x\mathbb{R}^{n_x}. \tag{1.1}$$

Recall that a solution of (1.1) is any locally absolutely continuous function $x(t)$, satisfying DI (1.1) for almost all t.

A differential inclusion (DI) (1.1) is further called *Filippov differential inclusion (DI)*, if the vector set $F(x)$ is non-empty, compact and convex for any x, and F is an upper-semicontinuous set function [31, 47]. The latter means that the maximal distance from the vectors of $F(x)$ to the vector set $F(y)$ vanishes as $x \to y$.

Solutions of the Filippov DI possess most of the well-known standard properties, like the local-solution existence for the Couchy problem, the solution extendability till the boundary of a compact and the continuous dependence on the *graph* of the DI [31]. Obviously, there is no solution uniqueness.

A differential equation (DE) $\dot{x} = f(x), x \in \mathbb{R}^{n_x}$, with a locally essentially bounded Lebesgue-measurable right-hand side is said to be understood *in the Filippov sense*, if its solutions are defined as the solutions of the special Filippov DI $\dot{x} \in K_F[f](x)$ with

$$K_F[f](x) = \bigcap_{\mu_L N=0} \bigcap_{\delta>0} \overline{co}\ f((x + B_\delta)\backslash N). \tag{1.2}$$

Here $\overline{co}$ denotes the convex closure operation, whereas μ_L is the Lebesgue measure. Formula (1.2) introduces the famous Filippov procedure [31]. In the non-autonomous case we introduce the fictitious coordinate t, $\dot{t} = 1$.

Whereas there are other definitions of solutions of the DE with discontinuous right-hand side, Filippov solutions satisfy all of them, i.e. constitute the minimal set of reasonably-defined solutions.

A point $x_0 \in \mathbb{R}^{n_x}$ is called the equilibrium of the Filippov DI (1.1), if $x(t) \equiv x_0$ is its solution. The equilibrium x_0 is called (Lyapunov) stable, if all solutions starting in some its vicinity at $t = 0$ are extendable till infinity in time, and for any $\varepsilon > 0$ there exists such $\delta > 0$ that each solution $x(t)$ satisfying $||x(0) - x_0|| < \delta$ satisfies $||x(t) - x_0|| < \varepsilon$ for any $t \geq 0$.

A stable equilibrium x_0 is called asymptotically stable (AS), if any solution $x(t)$ starting in some its vicinity satisfies $\lim_{t\to\infty} ||x(t) - x_0|| = 0$. It is globally AS if $\lim_{t\to\infty} ||x(t) - x_0|| = 0$ for any $x(0) \in \mathbb{R}^{n_x}$.

An AS equilibrium x_0 is called *FT stable* (FTS), if x_0 is AS, and for each initial condition $x(0)$ from a vicinity of x_0 there exists a number $T \geq 0$, such that $x(t) = x_0$ for any $t \geq T$. It is called *globally FTS*, if such T exists for any initial condition $x(0) \in \mathbb{R}^{n_x}$. The equilibrium x_0 is called *fixed-time (FxT) stable* (FxTS) [70], if it is globally FTS and the upper transient-time bound T can be chosen uniformly for all initial conditions.

A ball $x_0 + B_\varepsilon$ is called *FxT attractive*, if all trajectories converge to it in FxT, i.e. all solutions are extendable till infinity in time, and there exists such $T > 0$ that for any solution x the relation $x(t) \in x_0 + B_\varepsilon$ holds for any $t \geq T$.

Example 1 The origin 0 is a FxTS equilibrium of the scalar dynamic system $\dot{x} = -x^{1/3} - x^3$. Any ball $B_\varepsilon = \{x \in \mathbb{R} |\ |x| \leq \varepsilon\}$ is FxT attractive for the Filippov DI $\dot{x} \in -[1,2]x^3$. □

Globally (locally) AS Filippov DIs always have proper global (local) C^∞-smooth Lyapunov functions [17].

1.2.2 Weighted Homogeneity

Introduce the *weights (degrees)* $m_1, m_2, \ldots, m_{n_x} > 0$ of the coordinates $x_1, x_2, \ldots, x_{n_x}$ in $\mathbb{R}^{n_x}$, and denote $\deg x_i = m_i$. The simple linear transformation

$$d_\kappa(x) = (\kappa^{m_1} x_1, \kappa^{m_2} x_2, ..., \kappa^{m_{n_x}} x_{n_x}),\ \kappa \geq 0 \tag{1.3}$$

is called the *dilation* [6].

The function $f : \mathbb{R}^{n_x} \to \mathbb{R}^m$ is said to have the *homogeneity degree* (*weight*) $q \in \mathbb{R}$, $\deg f = q$, provided the identity $f(x) = \kappa^{-q} f(d_\kappa x)$ holds for any x and $\kappa > 0$.

We distinguish a vector function $f : \mathbb{R}^{n_x} \to \mathbb{R}^{n_x}, f : x \mapsto f(x) \in \mathbb{R}^{n_x}$, and a vector field $f : \mathbb{R}^{n_x} \to T\mathbb{R}^{n_x}, f : x \mapsto f(x) \in T_x\mathbb{R}^{n_x}$ [75]. In its turn the vector field $f(x) \in T_x\mathbb{R}^{n_x}$ is considered as a particular case of the vector-set field $F(x) \subset T_x\mathbb{R}^{n_x}$ for the vector set only containing one vector, $F(x) = \{f(x)\}$.

Correspondigly, a vector-set function $F(x) \subset \mathbb{R}^m$ is called *homogeneous* of the *homogeneity degree* (HD) $q \in \mathbb{R}$, if the identity $F(x) = d_\kappa^{-q} F(d_\kappa x)$ holds for any x and $\kappa > 0$ [47].

A vector-set field $F(x) \subset T_x\mathbb{R}^{n_x}$ (DI (1.1)) is called *homogeneous* of the *homogeneity degree* (HD) $q \in \mathbb{R}$, if the identity $F(x) = \kappa^{-q} d_\kappa^{-1} F(d_\kappa x)$ holds for any x and $\kappa > 0$ [47].

It follows from the latter definition that DI (1.1) is invariant with respect to the combined time-coordinate transformation

$$(t, x) \mapsto (\kappa^{-q} t, d_\kappa x), \quad \kappa > 0. \tag{1.4}$$

One can interprete $-q$ as the weight of the time t, $\deg t = -q$. In the case of a vector field (DE) the definition is reduced to the classical definition $\deg \dot{x}_i = \deg x_i - \deg t$ [6].

Any number can be considered as $\deg 0$, $\deg a = 0$ for any constant $a \neq 0$. The following simple rules of the homogeneous arithmetic are easily checked: $\deg A^a = a \deg A$, $\deg(AB) = \deg A + \deg B$, $\deg \frac{\partial}{\partial \alpha} A = \deg A - \deg \alpha$, $\deg \dot{A} = \deg A - \deg t$.

Any continuous positive-definite function of the HD 1 is called a *homogeneous norm*. We denote such norms by $||x||_h$. They are not real norms, but any two homogeneous norms $||\cdot||_h$ and $||\cdot||_{h*}$ are still equivalent in the sense that the inequalities $\gamma_* ||x||_{h*} \leq ||x||_h \leq \gamma^* ||x||_{h*}$ hold for some $\gamma_*, \gamma^* > 0$ and any x.

The following are two traditional homogeneous norms:

$$||x||_{h\infty} = \max_{1\le i\le n_x}\{|x_i|^{\frac{1}{m_i}}\},\ ||x||_{h\varpi} = (\sum_i |x|^{\frac{\varpi}{m_i}})^{\frac{1}{\varpi}}.$$

Note that the second homogeneous norm is continuously differentiable for $x \neq 0$, provided $\varpi > \max_i\{m_i\}$.

The weights and homogeneity degrees are defined up to proportionality. In other words, $\deg x_i = m_i, -\deg t = q$ can always be replaced with $\gamma m_i, \gamma q$ for any $\gamma > 0$. Also the HDs of all functions/fields/inclusions are multiplied by γ in that case. Obviously, such weight transformation does not preserve homogeneous norms.

A function is called *quasi-continuous* (QC) [48], if it is continuous everywhere except the origin. In particular, any continuous function is QC.

A homogeneous DI (1.1) is called AS (FTS, FxTS) if the origin 0 is its global AS (FTS, FxTS) equilibrium.

A set D_0 is called *homogeneously retractable* if $d_\kappa D_0 \subset D_0$ for any $\kappa \in [0,1]$.

A Filippov DI (1.1) is called *contractive* [47], if there exist positive numbers $T, \varepsilon > 0$, a retractable compact D_0 and a compact D_1, $0 \in D_1$, $D_1 + B_\varepsilon \subset D_0$, such that for any solution $x(t)$ the relation $x(0) \in D_0$ implies $x(T) \in D_1$.

A Filippov DI $\dot{x} \in \tilde{F}(x)$ is called a *small homogeneous perturbation* of the Filippov homogeneous DI $\dot{x} \in F(x)$ with the same dilation and the HD, if for some (small) $\varepsilon \geq 0$ the relation $\tilde{F}(x) \subset F(x) + B_\varepsilon$ holds whenever $x \in B_1$.

The following Theorem [54, 57, 38] summarizes stability features of DIs for arbitrary homogeneous degrees.

Theorem 1 *Let the Filippov DI* (1.1) *be homogeneous of the HD q. Then the asymptotic stability and the contractivity features are equivalent and robust with respect to small homogeneous perturbations.*

- *If* $q < 0$ *the asymptotic stability implies the FT stability, and the maximal (minimal) stabilization time is a well-defined upper (lower) semi-continuous function of the initial conditions [57]. Moreover, the FT stability of DI* (1.1) *implies that* $q < 0$.
- *If* $q = 0$ *the asymptotic stability is exponential.*
- *If* $q > 0$ *the asymptotic stability implies the FxT attractivity of any ball* B_ε, $\varepsilon > 0$. *The convergence to* 0 *is slower than exponential.*

Example 2 Consider any smooth DE $\dot{x} = f(x)$, $f(0) = 0$, $f'(0) = A$, $x \in \mathbb{R}^{n_x}$. Then $\dot{x} = f(x) \in \{Ax + \varepsilon||x||B_1\}$ holds for any $\varepsilon > 0$ in a sufficiently small vicinity of the origin.

One can consider the linear time-invariant system $\dot{x} = Ax$, $x \in \mathbb{R}^{n_x}$, $A \in \mathbb{R}^{n_x \times n_x}$, as a homogeneous Filippov DI $\dot{x} \in \{Ax\}$ of the HD 0 with $\deg x_i = 1$, $i = 1, ..., n_x$. Now, due to Theorem 1, the asymptotic stability of $\dot{x} = Ax$ implies the asymptotic stability of its small homogeneous perturbation $\dot{x} \in \{Ax + \varepsilon||x||B_1\}$, which, in its turn, implies the local asymptotic stability of $\dot{x} = f(x)$. □

The following theorem [6, 12] asserts that any AS homogeneous DI admits a smooth homogeneous Lyapunov function.

Theorem 2 *Let* (1.1) *be an AS Filippov homogeneous DI of the HD* q*. Then for any natural* l, k*,* $k > max(-q, l \max \deg x_i)$*, there exists a pair of continuous functions* $V, W : \mathbb{R}^{n_x} \to \mathbb{R}$*,* $V, W \in C^\infty(\mathbb{R}^{n_x} \setminus \{0\})$ *such that*

1. V *is positive definite and homogeneous,* $\deg V = k$*,* $V \in C^l(\mathbb{R}^{n_x})$*;*
2. W *is positive definite and homogeneous of degree* $k + q$*;*
3. $\max_{v \in F(x)} \nabla V(x) \cdot v \leq -W(x)$ *for all* $x \in \mathbb{R}^{n_x}$*.*

1.2.2.1 Accuracy of perturbed homogeneous DIs

Consider the retarded "noisy" perturbation of the AS Filippov homogeneous DI (1.1) of the negative homogeneity degree $q < 0$ [47]

$$\dot{x} \in F(x(t - [0, \tau]) + B_{h\varepsilon}),\ x \in \mathbb{R}^{n_x}, \tag{1.5}$$

where $\tau, \varepsilon \geq 0$, $B_{h\varepsilon} = \{x \in \mathbb{R}^{n_x} \mid ||x||_h \leq \varepsilon\}$.

In principle DI (1.5) requires some functional initial conditions for $t \in [-\tau, 0]$. The following result [46] requires some homogeneity assumptions on these conditions [28, 57] which are always satisfied provided the solutions do not depend on the solution prehistory for $t < 0$. That assumption usually holds in the case when the system is a combination of a smooth dynamic system with a digital dynamic controller based on discrete output sampling starting at $t = 0$.

So assume that the solutions of (1.5) do not depend on the values $x(t)$ for $t < 0$. Fix any homogeneous norm $|| \cdot ||_h$. Then the accuracy

$$x \in \gamma B_{h\rho},\ \rho = \max[\varepsilon, \tau^{-1/q}], \tag{1.6}$$

is established in FT for some $\gamma > 0$ independent of ε, τ and initial conditions.

If $q = 0$ that accuracy is established for $\rho = \varepsilon$ and any sufficiently small τ [28]. If $q > 0$ one also takes $\rho = \varepsilon$, but the initial value $x(0)$ and ε are to be uniformly bounded, whereas τ is to be sufficiently small for each fixed R, $x(0) \in B_R$ (it is the most "fragile" case [28], since the system can escape to infinity faster than any exponent [50]). A similar result also holds for the implicit Euler integration with the step τ [28].

1.3 Homogeneity approach to output regulation under uncertainty

Consider a dynamic system of the general form

$$\dot{x} = a(t, x) + b(t, x)u, \quad \sigma = \sigma(t, x), \tag{1.7}$$

where $x \in \mathbb{R}^{n_x}$, $u \in \mathbb{R}$, $\sigma : \mathbb{R}^{n_x+1} \to \mathbb{R}$ are the system control and the system output respectively. Smooth vector fields $a : \mathbb{R}^{n_x+1} \to T\mathbb{R}^{n_x}$, $b : \mathbb{R}^{n_x+1} \to T\mathbb{R}^n_x$ and the very dimension n_x are nowhere used and can be uncertain. Solutions of (1.7) are assumed forward complete, i.e. infinitely extendible in time, provided the control $u(t)$ is Lebesgue-measurable and bounded along the trajectory.

The system output function σ is sampled in real time and plays the role of the tracking deviation. The *control task* is to keep σ as small as possible.

The system (1.7) is assumed to possess a known relative degree r. It means [40] that the control for the first time explicitly appears in the rth total time derivative of σ, i.e.

$$\sigma^{(r)} = h(t,x) + g(t,x)u, \ \forall t, x: \ g(t,x) \neq 0, \tag{1.8}$$

where both $g, h : \mathbb{R}^{n_x+1} \to T\mathbb{R}$ are unknown smooth scalar vector fields, and g does never vanish. Moreover, the functions $\vec{\sigma}_{r-1} = (\sigma, ..., \sigma^{(r-1)})^T$ and t can always be extended to local coordinates in $\mathbb{R}^{n_x+1}$ [40].

According to the traditional SMC approach [46, 75] uncertain system dynamics (1.8) are extended to a quite certain controlled autonomous DI. For that end assume that

$$h(t,x) \in H(\vec{\sigma}_{r-1}), \ g(t,x) \in G(\vec{\sigma}_{r-1}) \tag{1.9}$$

for some convex compact upper-semicontinuous scalar (vector) set functions $H, G : \mathbb{R}^r \to T\mathbb{R}$. In the fixed coordinates $\vec{\sigma}_{r-1}$ these vector-set functions are naturally treated as numeric ones.

Apply some locally-essentially-bounded Lebesgue-measurable feedback control $u(\vec{\sigma}_{r-1})$. The resulting Filippov DI gets the form

$$\sigma^{(r)} \in H(\vec{\sigma}_{r-1}) + G(\vec{\sigma}_{r-1})K_F[u](\vec{\sigma}_{r-1}). \tag{1.10}$$

It is to become AS for a proper choice of control. Note that this approach requires the real-time estimation or availability of $\vec{\sigma}_{r-1}$.

The main idea is to make DI (1.10) homogeneous. Assign $\deg \sigma = 1$, and let the system HD be $q \in \mathbb{R}$, i.e. $\deg t = -q$. Then $\deg \sigma^{(i)} = 1 + iq$ holds for $i = 0, 1, ..., r-1$.

The required conditions $\deg \sigma^{(i)} > 0$ are ensured by the inequality $\deg \sigma^{(r)} = 1 + rq \geq 0$ which is in any case necessary for the feasibility of the system (Theorem 1 [57]). Thus, $q \geq -1/r$ is required. Also fix some homogeneous norm $||\cdot||_h$.

Assume that the set-functions H, G are homogeneous, $\deg H = 1 + rq$. Let also the control u be homogeneous, so that $\deg u = \deg K_F[u]$. Without losing the generality assume that $\deg G = 0$, i.e. $\deg u = 1 + rq$. This implies the inclusions

$$\begin{aligned} &h(t,x) \in H(\vec{\sigma}_{r-1}) \subseteq [-C, C]||\vec{\sigma}_{r-1}||_h^{1+rq}, \\ &g(t,x) \in G(\vec{\sigma}_{r-1}) \subseteq [K_m, K_M] \end{aligned} \tag{1.11}$$

for some constants $C \geq 0, K_m > 0, K_M \geq K_m$, and the DI [51]

$$\begin{aligned} &\sigma^{(r)} \in [-C, C]||\vec{\sigma}_{r-1}||_h^{1+rq} + [K_m, K_M]u, \\ &C \geq 0, \ 0 < K_m \leq K_M. \end{aligned} \tag{1.12}$$

Recall that the Filippov procedure $K_F[\cdot]$ is to be applied to u in order to produce a Filippov DI. The control u is assumed to be a Borel-measurable function of $\vec{\sigma}_{r-1}$ or of its dynamic estimation. The measurability in the sense of Borel is needed to ensure the Lebesgue measurability of the resulting control in the presence of Lebesgue-measurable noises. Note that all elementary functions are Borel-measurable.

The important case $q = -1/r$ corresponds to the standard high-order SMC (HOSMC) approach [46, 47]. In that case $\deg \sigma^{(r)} = 0$, and (1.12) gets the well-known form

$$\sigma^{(r)} \in [-C, C] + [K_m, K_M]u, \ \deg u = 0. \tag{1.13}$$

The corresponding assumptions $|h| \leq C$ and $g \in [K_m, K_M]$ are always at least locally true for some C, K_m, K_M.

In the case when (1.13) is AS, $q = -1/r$, it is also FT stable (Theorem 1), and the control feedback function $u(\vec{\sigma}_{r-1})$ is necessarily discontinuous at $\vec{\sigma} = 0$ for $C > 0$. The motion on the set $\vec{\sigma} = 0$ is said to be in the rth-order SM (r-SM), and the control is called rth-order SMC (r-SMC) [46, 47].

There are many homogeneous SM controllers solving the problem in the case $q = -1/r < 0$, $\deg u = 0$, some of them appear in [11, 24, 25, 39, 67, 68, 74, 75]. The recently established powerful method [18, 19] exploits the knowledge of a concrete homogeneous control Lyapunov function or builds it for the system $\sigma^{(r)} = u$ in order to generate an r-SM controller. Constructing a new control Lyapunov function becomes the initial non-trivial design step.

The alternative approach [51] presented below removes any differentiability conditions in the control construction and, correspondingly, yields significantly more controllers for any possible r and q.

1.4 Homogeneous control templates

We call two scalar functions $\omega, \varpi : \Omega \to \mathbb{R}$, $\Omega \subset \mathbb{R}^{n_\omega}$, *sign-equivalent* in Ω, if $\operatorname{sign} \omega(s) \equiv \operatorname{sign} \varpi(s)$ whenever $s \in \Omega$ and one of them is not zero.

Let the $(r-1)$th-order homogeneous DE

$$\sigma^{(r-1)} + \varphi_{r-1}(\vec{\sigma}_{r-2}) = 0, \tag{1.14}$$

be AS, and φ_{r-1} be continuous, $\deg \varphi_{r-1} = 1 + (r-1)q$. The following theorem extends the result [51] while exactly preserving its proof.

Theorem 3 *Let $q \geq -1/r$. Choose any homogeneous norm $||\vec{\sigma}_{r-1}||_h$, and let $\phi_r(\vec{\sigma}_{r-1})$ be any homogeneous quasi-continuous (QC) scalar function. Let ϕ_r also be sign-equivalent to $\sigma^{(r-1)} + \varphi_{r-1}(\vec{\sigma}_{r-2})$ for $\vec{\sigma}_{r-1} \neq 0$. Consider the homogeneous controls of the form*

$$u = \alpha U_r(\vec{\sigma}_{r-1}), \tag{1.15}$$

where $\alpha > 0$, and U_r is defined by one of the formulas

$$U_r(\vec{\sigma}_{r-1}) = -||\vec{\sigma}_{r-1}||_h^{1+qr-\deg\phi_r}\phi_r(\vec{\sigma}_{r-1}), \quad (1.16)$$

$$U_r(\vec{\sigma}_{r-1}) = -||\vec{\sigma}_{r-1}||_h^{1+qr}\operatorname{sign}\phi_r(\vec{\sigma}_{r-1}). \quad (1.17)$$

Then for any sufficiently large $\alpha > 0$ *these controllers asymptotically stabilize DI* (1.12). *In particular the homogeneous DE*

$$\sigma^{(r)} + \varphi_r(\vec{\sigma}_{r-1}) = 0,\ \varphi_r(\vec{\sigma}_{r-1}) = -\alpha U_r(\vec{\sigma}_{r-1}), \quad (1.18)$$

is AS for any sufficiently large α. *The function* φ_r *is continuous for* $q > -1/r$, *if* U_r *is taken in the form* (1.16).

Control function (1.16) *is QC (i.e. discontinuous only at* $\vec{\sigma}_{r-1} = 0$*) for* $q = -1/r$. *It is continuous for* $q > -1/r$, *provided* $U_r(0) = 0$ *is assigned. DI* (1.12) *(in particular* (1.18)*) is FT stable for* $q < 0$, *and exponentially stable for* $q = 0$. *If* $q > 0$ *any ball* B_ε *attracts solutions in FxT.*

When applied to the general system (1.7) the controllers can be multiplied by any locally bounded Lebesque-measurable function $k(t, x) \geq 1$ without losing the convergence of σ to zero.

The chattering of the QC r-SM controller (1.15), (1.16), obtained in the case $q = -1/r$, is much lower compared with (1.15), (1.17) [48]. Also, in spite of controller (1.15), (1.17) looking as a classical SM controller, it does not keep the SM $\phi_r(\vec{\sigma}_{r-1}) = 0$, since $\phi_r(\vec{\sigma}_{r-1})$ in general features infinite gradients.

1.4.1 Recursion in the relative degree

Actually, under the condition $q \geq -1/r$, Theorem 3 establishes a recursion from the $(r-1)$th-order AS DE (1.14) to the new rth-order AS DE (1.18).

In the sequel we use that $A + B$ and $\lfloor A \rceil^\gamma + \lfloor B \rceil^\gamma$ are sign-equivalent for any $A, B \in \mathbb{R}$ and $\gamma > 0$.

The initial step. Let $q \geq -1$. The AS DE (1.14) of the order 1 can always be chosen as

$$\dot{\sigma} + \beta_0 \lfloor \sigma \rceil^{1+q} = 0,\ \beta_0 > 0. \quad (1.19)$$

In order to recursively construct a homogeneous stabilizer for $r = 2$ one will need $q \geq -1/2$.

The recursive step. Let an $(r-1)$th-order AS DE (1.14) be given, $q \geq -1/r$. Choose two arbitrary homogeneous norms $||\cdot||_h, ||\cdot||_{h*}$, some $m > 0$, and any QC function $\theta(s)$, $\theta : \mathbb{R} \setminus \{0\} \to \mathbb{R}$, sign-equivalent to s, e.g. $\theta(s) = (s + \sin s)^{-1}$. Then the following are only three of the simplest choices for $\phi_r(\vec{\sigma}_{r-1})$:

$$\begin{aligned}
&1.\ \phi_r(\vec{\sigma}_{r-1}) = \lfloor \sigma^{(r-1)} + \varphi_{r-1} \rceil^m, && \deg\varphi_r = m > 0,\\
&2.\ \phi_r(\vec{\sigma}_{r-1}) = \lfloor \sigma^{(r-1)} \rceil^m + \lfloor \varphi_{r-1} \rceil^m, && \deg\varphi_r = m > 0,\\
&3.\ \phi_r(\vec{\sigma}_{r-1}) = \theta\left(\frac{\lfloor \sigma^{(r-1)} + \varphi_{r-1} \rceil^m}{||\vec{\sigma}_{r-1}||_h^{m(1+(r-1)q)}}\right), && \deg\varphi_r = 0.
\end{aligned} \quad (1.20)$$

Alternatively one, for example, can take the function

$$\phi_r(\vec{\sigma}_{r-1}) = \\ |\sigma^{(r-1)} + \varphi_{r-1}|^{m_1} \left| \lfloor \sigma^{(r-1)} \rceil^{m_2} + \lfloor \varphi_{r-1} \rceil^{m_2} \right| \theta \left(\frac{\lfloor \sigma^{(r-1)} \rceil^{m_3} + \lfloor \varphi_{r-1} \rceil^{m_3}}{||\vec{\sigma}_{r-1}||_h^{m_3(1+(r-1)q)}} \right)$$

with $\deg \phi_r = m_1 + m_2$, $m_2, m_3 > 0$, $m_1 + m_2 \geq 0$, etc. There are, obviously, infinitely many such constructions for each $r \geq 2$.

Now, according to Theorem 3, from (1.16), (1.17) obtain the new homogeneous controls (1.15) of the order r,

$$u_r = -\alpha ||\vec{\sigma}_{r-1}||_{h*}^{1+qr-\deg \phi_r} \phi_r(\vec{\sigma}_{r-1}), \\ u_r = -\alpha ||\vec{\sigma}_{r-1}||_{h*}^{1+qr} \operatorname{sign} \phi_r(\vec{\sigma}_{r-1}), \tag{1.21}$$

and the rth-order AS DE (1.18)

$$\sigma^{(r)} + \beta_{r-1} ||\vec{\sigma}_{r-1}||_{h*}^{1+qr-\deg \phi_r} \phi_r(\vec{\sigma}_{r-1}) = 0. \tag{1.22}$$

The new equation contains uncertain parameters of the auxiliary function ϕ_r, as well as the uncertain parameter β_{r-1}. It is natural to call (1.21) *a controller template*. If $q \geq -1/(r+1)$ one can now perform one more recursive step, etc.

In general one needs $r-1$ recursive steps to develop a controller of the order r, provided $q \geq -1/r$. But the first step (1.19) is trivial, since any $\beta_0 > 0$ is admissible. It is reasonable to immediately assign proper values to additional design parameters which appear at each recursion step. Usually it is done by simulation of (1.22).

1.4.1.1 HOSMC template development

The most practical special case is definitely the case of SM control. Let the relative degree be $r \geq 1$. Then the corresponding system HD is $-1/r$ and $\deg \sigma^{(r)} = \deg u = 0$. In that case it is usually convenient to proportionally change all the weights, getting $q = -1$, $\deg \sigma^{(i)} = r - i$ for $i = 0, 1, ..., r$, $\deg t = 1$ (the r-sliding homogeneity [47]).

A number of r-SM controllers are readily available, and their parameters are known in advance at least till $r = 5$ [24, 75]. Note that the parameter α from (1.15) defines the control magnitude and is only assigned at the last practical control-design stage.

The presented control template development is so simple that one can develop a new r-SM controller for each practical application (Section 1.9.1). In that case the first recursion step almost always employs $\dot{\sigma} + \beta_0 \lfloor \sigma \rceil^{\frac{r-1}{r}} = 0$, though one can, for example, take "exotic" $\dot{\sigma} + \beta_0 (2 + \operatorname{sign} \sigma) \lfloor \sigma \rceil^{\frac{r-1}{r}} = 0$ instead. Fix some $\beta_0 > 0$.

At the next step one has already infinitely-many variants. Any equation of the form $\ddot{\sigma} + \beta_1 \phi(\sigma, \dot{\sigma}) = 0$ is admissible, provided $\deg \phi = \deg \ddot{\sigma}$, ϕ is QC and sign-equivalent to $\dot{\sigma} + \beta_0 \lfloor \sigma \rceil^{\frac{r-1}{r}}$.

For example,

$$\ddot{\sigma} + \beta_1 \tan \left(\frac{\dot{\sigma} + \beta_0 \lfloor \sigma \rceil^{\frac{r-1}{r}}}{|\dot{\sigma}| + \beta_0 |\sigma|^{\frac{r-1}{r}}} \right) \left| \lfloor \dot{\sigma} \rceil^{\frac{1}{2}} + \beta_0^{\frac{1}{2}} \lfloor \sigma \rceil^{\frac{r-1}{2r}} \right|^{\frac{2r-4}{r-1}} = 0$$

can be taken. The equation is AS for any sufficiently large $\beta_1 > 0$ to be assigned by simulation. The recursion process proceeds then to an AS equation for $\dddot{\sigma}$, etc. A complete design for $r = 3, 4$ is demonstrated in the simulation Section 1.9.1.

1.5 Filtering SM-based differentiation

The practical realization of the r-SM controllers developed in Section 1.4.1.1 requires the real-time estimation of the derivatives $\vec{\sigma}_{r-1}$. Some popular observation methods applied in that context are based on high-gain observers [5] and SMs [75]. In the following we present some modern methods of SM-based observation featuring fast robust exact derivatives' estimation while keeping high accuracy in the presence of large and even unbounded noises, provided they are small in average.

1.5.1 Homogeneous differentiation

1.5.1.1 Standard differentiator

The control approach to the nth-order differentiation of a noisy sampled function $f_0(t)$ suggests constructing an observer for the disturbed integrator chain $y^{(n+1)} = \xi(t)$ with the output y and the unknown disturbance/input $\xi = f_0^{(n+1)}(t)$. Its outputs z_i, $i = 0, ..., n$, are to approximate the $y^{(i)}(t)$ in spite of $y = f_0(t)$ being sampled with some noise and $\xi(t)$ being unknown. The problem is very old and is known to be ill posed, if no restrictions are imposed on ξ.

Let the input $f(t)$ take the form $f(t) = f_0(t) + \eta(t) \in \mathbb{R}$, where $\eta(t)$ is a Lebesgue-measurable bounded noise, $|\eta(t)| < \varepsilon_0$, and $f_0(t)$ is an n-times differentiable unknown function to be restored together with its n derivatives in spite of the unknown measurement noise intensity ε_0. The last derivative $f_0^{(n)}$ is assumed to have a known Lipschitz constant $L > 0$, which means that $f_0^{(n+1)}(t) \in [-L, L]$ holds for almost all t. It is further denoted as $f_0 \in \mathrm{Lip}_n L$.

The general differentiator [5, 46] is usually of the form

$$\begin{aligned} &\dot{z}_i = \varphi_i(z_0 - f(t)) + z_{i+1},\ i = 0, ..., n-1, \\ &\dot{z}_n = \varphi_n(z_0 - f(t)), \end{aligned} \tag{1.23}$$

where φ_i is a scalar function, $z_i \in \mathbb{R}$. The system is understood in the Filippov sense [31] to allow discontinuities of φ_i. The equivalent recursive form of (1.23) is

$$\begin{aligned} &\dot{z}_0 = \varphi_i(z_0 - f(t)) + z_1, \\ &\dot{z}_i = \varphi_i(z_i - \dot{z}_{i-1}) + z_{i+1},\ i = 1, ..., n-1, \\ &\dot{z}_n = \varphi_n(z_0 - f(t)). \end{aligned} \tag{1.24}$$

Assuming the noise is absent (i.e. $\varepsilon_0 = 0$), subtracting $f_0^{(i+1)}$ from both sides of (1.23), and denoting $\sigma_i = z_i - f_0^{(i)}$, derive

$$\begin{aligned} &\dot{\sigma}_i = \varphi_i(\sigma_0) + \sigma_{i+1},\ i = 0, ..., n-1 \\ &\dot{\sigma}_n \in \varphi_n(\sigma_0) + [-L, L], \end{aligned} \tag{1.25}$$

which is a DI in the error space $\vec{\sigma}_n$. DI (1.23) becomes homogeneous and FT stable for properly chosen functions φ_i.

The "standard" nth-order homogeneous SM-based differentiator [46] has the form

$$\begin{aligned} \dot{z}_0 \quad &= -\tilde{\lambda}_n L^{\frac{1}{n+1}} \lfloor z_0 - f \rceil^{\frac{n}{n+1}} + z_1, \\ \dot{z}_1 \quad &= -\tilde{\lambda}_{n-1} L^{\frac{2}{n+1}} \lfloor z_0 - f \rceil^{\frac{n-1}{n+1}} + z_2, \\ &\dots \\ \dot{z}_{n-1} &= -\tilde{\lambda}_1 L^{\frac{n}{n+1}} \lfloor z_0 - f \rceil^{\frac{1}{n+1}} + z_n, \\ \dot{z}_n \quad &= -\tilde{\lambda}_0 L \operatorname{sign}(z_0 - f), \end{aligned} \tag{1.26}$$

where the parameters $\tilde{\lambda}_i > 0$ of the differentiator (1.28) are to be chosen in advance for each $n,\ i = 0, 1, 2, ..., n$.

A proper choice of the parameters $\tilde{\lambda}_i$ renders the error dynamics FTS. Correspondingly, in the absence of noises the equalities $z_i = f_0^{(i)}$ are established in FT.

For the future usage introduce the number n_d currently equal to the differentiation order n. Then in the presence of a sampling noise with the maximal magnitude ε_0 the accuracy

$$\left| z_i - f_0^{(i)} \right| \leq \gamma_i L \left(\tfrac{\varepsilon_0}{L} \right)^{\frac{(n_d - i + 1)}{(n_d + 1)}} \tag{1.27}$$

is obtained in FT for some $\gamma_i \geq 1$ only depending on the coefficients $\vec{\tilde{\lambda}}_n$.

Whereas γ_i depend on the parameters $\tilde{\lambda}_i$ of (1.26), the asymptotics structure (1.27) (i.e. the powers) is fixed and cannot be improved by any differentiation algorithm exact on functions $f_0 \in \mathrm{Lip}_n(L)$ [45]. Moreover, it can be shown that $\gamma_i \geq 2^{i/(n_d+1)}$ [60]. Therefore, an n_dth-order differentiator of *any nature* is called asymptotically optimal, if it provides for the steady-state accuracy (1.27) for all signals and noises satisfying the above assumptions [60].

It is not simple to properly choose the differentiator parameters for each n. The task is facilitated by employing its recursive form [46]

$$\begin{aligned} \dot{z}_0 &= -\lambda_n L^{\frac{1}{n+1}} \lfloor z_0 - f(t) \rceil^{\frac{n}{n+1}} + z_1, \\ \dot{z}_1 &= -\lambda_{n-1} L^{\frac{1}{n}} \lfloor z_1 - \dot{z}_0 \rceil^{\frac{n-1}{n}} + z_2, \\ &\ldots \\ \dot{z}_{n-1} &= -\lambda_1 L^{\frac{1}{2}} \lfloor z_{n-1} - \dot{z}_{n-2} \rceil^{\frac{1}{2}} + z_n, \\ \dot{z}_n &= -\lambda_0 L \,\mathrm{sign}(z_n - \dot{z}_{n-1}), \end{aligned} \tag{1.28}$$

for some positive $\lambda_i > 0$, $i = 0, 1, ..., n$. Excluding $\dot{z}_i$ reduce (1.28) to the general structure (1.23) and the standard form (1.26). It is easily verified that $\tilde{\lambda}_0 = \lambda_0, \tilde{\lambda}_n = \lambda_n$, and $\tilde{\lambda}_i = \lambda_i \tilde{\lambda}_{i+1}^{\frac{i}{i+1}}, i = n-1, n-2, ..., 1$.

In the case $f(t) \equiv 0$ systems (1.26) and (1.28) become homogeneous of the HD -1 with $\deg t = 1$, $\deg z_i = \deg \sigma_i = n - i + 1$, $i = 0, ..., n$.

An infinite sequence of parameters $\overrightarrow{\lambda} = \{\lambda_0, \lambda_1, ...\}$ can be built [46], providing coefficients $\tilde{\lambda}_i$ of (1.26) for all natural n. For this end one simply starts with any $\lambda_0 > 1$ and recursively adds a sufficiently large value $\lambda_n > 0$ for each $n = 1, 2, ...$.

The parameters are surprisingly easily found by simulation. In particular, $\overrightarrow{\lambda} = \{1.1, 1.5, 2, 3, 5, 7, 10, 12, 14, 16, 20, 26, 32, ...\}$ are well checked for $n \leq 12$. Note that a shorter sequence up to $n = 7$ has been published in [58, 60], while a sequence till $n = 5$ was the first one to appear in [46]. The corresponding parameters $\tilde{\lambda}_i$ are listed in Table 1.26. Alternative parameters are provided in Section 1.5.2 by another sequence $\overrightarrow{\lambda}$ (1.37). It is always assumed in the following that the parameters λ_i are properly chosen, so that (1.26) is finite time stable.

Table 1.1 Parameters $\tilde{\lambda}_0, \tilde{\lambda}_1, ..., \tilde{\lambda}_n$ of differentiator (1.26) for $n = 0, 1, ..., 12$

0	1.1												
1	1.1	1.5											
2	1.1	2.12	2										
3	1.1	3.06	4.16	3									
4	1.1	4.57	9.30	10.03	5								
5	1.1	6.75	20.26	32.24	23.72	7							
6	1.1	9.91	43.65	101.96	110.08	47.69	10						
7	1.1	14.13	88.78	295.74	455.40	281.37	84.14	12					
8	1.1	19.66	171.73	795.63	1703.9	1464.2	608.99	120.79	14				
9	1.1	26.93	322.31	2045.8	6002.3	7066.2	4026.3	1094.1	173.72	17			
10	1.1	36.34	586.78	5025.4	19895	31601	24296	8908	1908.5	251.99	20		
11	1.1	48.86	1061.1	12220	65053	138954	143658	70830	20406	3623.1	386.7	26	
12	1.1	65.22	1890.6	29064	206531	588869	812652	534837	205679	48747	6944.8	623.30	32

1.5.1.2 Filtering differentiators

The following filter/observer is build on the basis of the standard differentiator (1.26) and, remaing exact, is capable of filtering out *unbounded* sampling noises.

Introduce the number $n_f \geq 0$ which is further called *the filtering order*. Correspondingly, n_d is further called *the differentiation order*. Let $n_d, n_f \geq 0$, where n_f

is called *the filtering order*. The filtering differentiator is defined by the new form

$$\begin{aligned}
&\dot{w}_1 = -\tilde{\lambda}_{n_d+n_f} L^{\frac{1}{n_d+n_f+1}} \lfloor w_1 \rceil^{\frac{n_d+n_f}{n_d+n_f+1}} + w_2,\\
&\quad \dots\\
&\dot{w}_{n_f-1} = -\tilde{\lambda}_{n_d+2} L^{\frac{n_f-1}{n_d+n_f+1}} \lfloor w_1 \rceil^{\frac{n_d+2}{n_d+n_f+1}} + w_{n_f},\\
&\dot{w}_{n_f} = -\tilde{\lambda}_{n_d+1} L^{\frac{n_f}{n_d+n_f+1}} \lfloor w_1 \rceil^{\frac{n_d+1}{n_d+n_f+1}} + w_{n_f+1},\\
&w_{n_f+1} = z_0 - f(t),
\end{aligned} \tag{1.29}$$

$$\begin{aligned}
&\dot{z}_0 = -\tilde{\lambda}_{n_d} L^{\frac{n_f+1}{n_d+n_f+1}} \lfloor w_1 \rceil^{\frac{n_d}{n_d+n_f+1}} + z_1,\\
&\quad \dots\\
&\dot{z}_{n_d-1} = -\tilde{\lambda}_1 L^{\frac{n_d+n_f}{n_d+n_f+1}} \lfloor w_1 \rceil^{\frac{1}{n_d+n_f+1}} + z_{n_d},\\
&\dot{z}_{n_d} = -\tilde{\lambda}_0 L \,\mathrm{sign}(w_1), \; |f_0^{(n_d+1)}| \le L.
\end{aligned} \tag{1.30}$$

Parameters $\tilde{\lambda}_i$, $i = 0, 1, ..., n$, $n = n_d + n_f$, of (1.26) and (1.29), (1.30) coincide and can be taken from Table 1.1.

For $n_f = 0$ the fictitious variable w_{n_f+1} turns into w_1, DEs of (1.29) disappear and (1.30) turns into the standard differentiator (1.26). The assumptions on the input signal are the same. It was recently shown [59] that the steady state accuracies

$$\begin{aligned}
&|w_1| \le \gamma_{w_1} L \rho^{n_f+n_d+1},\\
&\left| z_i - f_0^{(i)}(t) \right| \le \gamma_i L \rho^{n_d+1-i}, \; i = 0, ..., n_d
\end{aligned} \tag{1.31}$$

$$|w_j| \le \gamma_{w_j} L \rho^{n_d+n_f+2-j}, \; j = 2, ..., n_f, \tag{1.32}$$

are in FT established for

$$\rho = (\varepsilon_0/L)^{\frac{1}{(n_d+1)}}, \tag{1.33}$$

and some γ_{w_1}, $\gamma_{w_j}, \gamma_i > 0$ only depending on the choice of $\lambda_0, ..., \lambda_{n_d+n_f}$. It means that (1.29), (1.30) describe *an alternative asymptotically optimal n_dth-order differentiator*.

This differentiator has new significant filtering properties to be presented in Section 1.7. The accuracy estimation (1.32) is singled out, since it does not hold for the corresponding ρ in the presence of large noises considered there.

1.5.2 Hybrid (bi-homogeneous) filtering differentiators

As we have seen above the usual requirement of HOSM-based n_dth-order differentiation is that the n_dth derivative $f_0^{(n_d)}$ has a known Lipschitz constant $L > 0$. Presented homogeneous differentiators solve the problem both robustly and exactly. Unfortunately, a well-known drawback of these differentiators is the low convergence rate for large initial errors.

After the differentiator coefficients are fixed, the Lipschitz constant L actually remains the only adjustable parameter of the standard HOSM-based differentiator [46]. Thus, it is natural to try tuning that parameter in order to accelerate the convergence, while keeping the same steady state accuracy (1.31), (1.33).

Unfortunately, filtering and standard differentiators with variable parameter L in general converge only locally [55, 58] (global convergence is preserved for monotonously growing differentiable $L(t)$ [64]).

These issues are settled by the so-called hybrid differentiator [58] of the general structure (1.24). New quasi-linear terms are for this end added to the recursive form (1.28) of the differentiator producing a hybrid differentiator combining the features of the homogeneous differentiator (1.28) and a linear filter similar to the high-gain observer (HGO) [5], but with gains which are not to be large.

The following is its further modification to the hybrid filtering differentiator [37],

$$\begin{aligned}
\dot{w}_1 &= -\lambda_{n_d+n_f} L^{\frac{1}{n_d+n_f+1}} \lfloor w_1 \rceil^{\frac{n_d+n_f}{n_d+n_f+1}} \\
&\qquad\qquad -\mu_{n_d+n_f} M w_1 + w_2, \\
&\cdots \\
\dot{w}_{n_f-1} &= -\lambda_{n_d+2} L^{\frac{1}{n_d+3}} \lfloor w_{n_f-1} - \dot{w}_{n_f-2} \rceil^{\frac{n_d+2}{n_d+3}} \\
&\qquad -\mu_{n_d+2} M (w_{n_f-1} - \dot{w}_{n_f-2}) + w_{n_f}, \\
\dot{w}_{n_f} &= -\lambda_{n_d+1} L^{\frac{1}{n_d+2}} \lfloor w_{n_f} - \dot{w}_{n_f-1} \rceil^{\frac{n_d+1}{n_d+2}} \\
&\qquad -\mu_{n_d+1} M (w_{n_f} - \dot{w}_{n_f-1}) + z_0 - f(t),
\end{aligned} \tag{1.34}$$

$$\begin{aligned}
\dot{z}_0 &= -\lambda_{n_d} L^{\frac{1}{n_d+1}} \lfloor z_0 - f(t) - \dot{w}_{n_f} \rceil^{\frac{n_d}{n_d+1}} \\
&\qquad -\mu_{n_d} M (z_0 - f(t) - \dot{w}_{n_f}) + z_1, \\
\dot{z}_1 &= -\lambda_{n_d-1} L^{\frac{1}{n_d}} \lfloor z_1 - \dot{z}_0 \rceil^{\frac{n_d-1}{n_d}} \\
&\qquad -\mu_{n_d-1} M (z_1 - \dot{z}_0) + z_2, \\
&\cdots \\
\dot{z}_{n_d} &= -\lambda_0 L \lfloor z_{n_d} - \dot{z}_{n_d-1} \rceil^0 \\
&\qquad -\mu_0 M (z_{n_d} - \dot{z}_{n_d-1})
\end{aligned} \tag{1.35}$$

where $\vec{\lambda}_{n_d+n_f}$ and $\vec{\mu}_{n_d+n_f}$ are some properly chosen positive numbers.

This differentiator converges in FT and exactly, provided $|f_0^{(n_d+1)}(t)| \leq L(t)$ and $|\dot{L}/L| \leq M$ hold. The convergence rate is exponential to any vicinity of the error space origin, and is easily regulated by M [58]. The accuracy is covered by Theorem 4 [37] in the sequel.

The hybrid filtering differentiator (1.40), (1.38) turns into the "standard" hybrid differentiator [58] for $n_f = 0$, into the filtering differentiator (1.29), (1.30) for $M = 0$, into the "standard" differentiator (1.23) for $n_f = 0,\ M = 0$, and into the linear HGO [5] for $n_f = 0$, $L = 0$, $M >> 1$. The coefficients of the resulting HGO are $\mu_{n_d}, \mu_{n_d}\mu_{n_d-1}, \ldots, \mu_{n_d}\mu_{n_d-1}\cdots\mu_0$ from the top-down and correspond to the characteristic polynomial

$$s^{n_d+1} + \mu_{n_d} s^{n_d} + \mu_{n_d}\mu_{n_d-1} s^{n_d-1} + \ldots + \mu_{n_d}\mu_{n_d-1}\cdots\mu_0. \tag{1.36}$$

Also here one can construct infinite double sequence of parameters valid for any $n_d + n_f$ [37]. In particular, the sequence

$$\{(\lambda_0, \mu_0), (\lambda_1, \mu_1), ...\} = (1.1, 2), (1.5, 3), (2, 4), (3, 7), (5, 9), (7, 13), (10, 19), \\ (12, 23), (15, 42), (21, 43), (25, 79), (39, 98), (78, 116), \dots \quad (1.37)$$

has been experimentally validated for $n \leq 12$ and can be extended up to $n_d + n_f = n = \infty$. Set (1.37) extends the parametric set valid till $n = 7$ which has been published in [7, 58].

It has been proved ([58]) that the sequence λ_i is also valid for use in the standard and filtering differentiators, but the authors prefer parameters from Tab. 1.1 in that case. Note that parameters μ_i produce Hurwitz polynomials (1.36) for each $n_d = 0, 1, ...$ [58].

Introduce the functions

$$\varphi_{i,n}(s, L) = \lambda_{n-i} L^{\frac{1}{n-i+1}} |s|^{\frac{n-i}{n-i+1}} \operatorname{sign} s + \mu_{n-i} M s, \ i = 0, ..., n. \quad (1.38)$$

Then the proposed hybrid filtering differentiator gets the form

$$\begin{aligned} &\dot{w}_1 = v_{w1} = -\varphi_{0,n_d+n_f}(w_1, L) + w_2, \\ &\dot{w}_2 = v_{w2} = -\varphi_{1,n_d+n_f}(w_2 - v_{w1}, L) + w_3, \\ &... \\ &\dot{w}_{n_f} = v_{wn_f} = -\varphi_{n_f,n_d+n_f}(w_{n_f} - v_{wn_f-1}, L) + z_0 - f(t). \end{aligned} \quad (1.39)$$

$$\begin{aligned} &\dot{z}_0 = v_0 = -\varphi_{n_f+1,n_d+n_f}(z_0 - v_{wn_f} - f(t), L) + z_1, \\ &\dot{z}_1 = v_1 = -\varphi_{n_f+2,n_d+n_f}(z_1 - v_0, L) + z_2, \\ &... \\ &\dot{z}_n = v_{n_d} = -\varphi_{n_d+n_f,n_d+n_f}(z_n - v_{n_d-1}, L). \end{aligned} \quad (1.40)$$

The recursive form (1.39), (1.40) is identically rewritten in the standard dynamic-system form

$$\begin{aligned} &\dot{w}_1 = -\varphi_{0,n_d+n_f}(w_1, L) + w_2, \\ &\dot{w}_2 = -\varphi_{1,n_d+n_f}(\varphi_{0,n_d+n_f}(w_1, L), L) + w_3, \\ &... \\ &\dot{w}_{n_f} = -\varphi_{n_f,n_d+n_f}(\varphi_{n_f-1,n_d+n_f}(...(w_1, L)..., L), L) + z_0 - f(t), \end{aligned} \quad (1.41)$$

$$\begin{aligned} &\dot{z}_0 = -\varphi_{n_f+1,n_d+n_f}(\varphi_{n_f,n_d+n_f}(...(w_1, L)..., L), L) + z_1, \\ &... \\ &\dot{z}_n = -\varphi_{n_d+n_f,n_d+n_f}(\varphi_{n_d+n_f-1,n_d+n_f}(...(w_1, L)..., L), L), \end{aligned} \quad (1.42)$$

but only the recursive form is usable in practice.

1.6 Discretization of differentiators and controllers

In practice any observer is a discrete computer-based system processing a discretely sampled noisy output of a continuous-time system. Thus, the differential equations are to be replaced with their numeric real-time integration. One also cannot apply standard numeric integration methods, since the considered observer is a discontinuous dynamic system.

The simplistic Euler integration works, but significantly destroys the theoretical accuracy [7], [62]. The right discretization is to produce homogeneous discrete error dynamics analogous to that of the continuous-time sampling case.

The same problems naturally appear in the implementation of output-feedback systems. In such a case also the controller is computer based.

1.6.1 Discretization of differentiators

Let t_j be the sampling instants, $0 < t_{j+1} - t_j = \tau_j \leq \tau$, $j = 0, 1, ...$, $\lim_{j\to\infty} t_j = \infty$. Though the sampling steps are assumed bounded, their upper bound τ does not need to be available.

Notation. Denote $\delta_j A = A(t_{j+1}) - A(t_j)$ for any function A.

The proposed discrete differentiator

$$\begin{array}{l} \delta_j w_1 = \varphi_{0,n_d+n_f}(w_1(t_j), L)\tau_j + w_2(t_j)\tau_j, \\ \delta_j w_2 = \varphi_{1,n_d+n_f}(w_2(t_j) - v_{w1}(t_j), L)\tau_j + w_3(t_j)\tau_j, \\ \dots, \\ \delta_j w_{n_f} = \varphi_{n_f,n_d+n_f}(w_{n_f}(t_j) - v_{wn_f-1}(t_j), L)\tau_j + (z_0(t_j) - f(t_j))\tau_j, \end{array} \tag{1.43}$$

$$\begin{array}{l} \delta_j z_0 = \varphi_{n_f+1,n_d+n_f}(z_0(t_j) - f(t_j) - v_{wn_f}(t_j), L)\tau_j + \sum\limits_{i=1}^{n_d} \frac{z_i}{i!}\tau_j^i, \\ \delta_j z_1 = \varphi_{n_f+2,n_d+n_f}(z_1(t_j) - v_0(t_j), L)\tau_j + \sum\limits_{i=2}^{n_d} \frac{z_i}{(i-1)!}\tau_j^{i-1}, \\ \dots, \\ \delta_j z_{n_d-1} = \varphi_{n_f+2,n_d+n_f}(z_{n_d-1}(t_j) - v_{n_d-2}(t_j), L)\tau_j + z_{n_d}(t_j)\tau_j, \\ \delta_j z_{n_d} = \varphi_{n_f+2,n_d+n_f}(z_{n_d}(t_j) - v_{n_d-1}(t_j), L)\tau_j. \end{array} \tag{1.44}$$

has additional Taylor-like terms. Functions $v_i, v_{wj}, \varphi_{i,n}$ are defined in (1.39), (1.40) and (1.38).

Denote the (n_f, n_d)th order filtering hybrid differentiator (1.38), (1.41), (1.42) by $(\dot{w}, \dot{z})^T = D_{n_f,n_d}(w, z_0 - f, z, L)$, where the difference $z_0 - f(t)$ is singled out. Then the above discrete differentiator (1.43), (1.44) gets the form

$$\delta_j (w, z)^T = D_{n_f,n_d}(w(t_j), z_0(t_j) - f(t_j), z(t_j), L)\tau_j + T_{n_f,n_d}(z(t_j), \tau_j), \tag{1.45}$$

$$\begin{bmatrix} T_0 \\ \dots \\ T_{n_f-1} \\ T_{n_f} \\ \dots \\ T_{n_f+i} \\ \dots \\ T_{n_f+n_d-2} \\ T_{n_f+n_d-1} \\ T_{n_f+n_d} \end{bmatrix} = \begin{bmatrix} 0 \\ \dots \\ 0 \\ \frac{1}{2!} z_2(t_j)\tau_j^2 + \ldots + \frac{1}{n_d!} z_{n_d}(t_j)\tau_j^{n_d} \\ \dots \\ \sum_{s=i+2}^{n_d} \frac{1}{(s-i)!} z_s(t_j)\tau_j^{s-i} \\ \dots \\ \frac{1}{2!} z_{n_d}(t_j)\tau_j^2 \\ 0 \\ 0 \end{bmatrix} \quad (1.46)$$

Here $T_{n_f,n_d} \in \mathbb{R}^{n_f+n_d+1}$. In particular $T_{n_f,0}(w,z,\tau) = 0 \in \mathbb{R}^{n_f+1}$, $T_{n_f,1}(w,z,\tau) = 0 \in \mathbb{R}^{n_f+2}$.

The following theorem easily follows from the similar result on hybrid differentiators [7, 58]. The limit case $\tau = 0$ is formally covered in that theorem as the replacement of (1.45) with the continuous-time hybrid filtering differentiator (1.34), (1.35) processing the signal f_0 corrupted by the Lebesgue-measurable noise $\eta(t)$.

Theorem 4 *Under the assumption that* $|f_0^{(n_d+1)}(t)| \leq L(t)$*, let the absolutely continuous function L(t) satisfy* $|\dot{L}/L| \leq M$*, and the sampling noise satisfy* $|\eta(t)/L| \leq \hat{\varepsilon}$*. Then differentiator* (1.45) *in FT provides for the accuracy* (1.31)*,* (1.32) *with* $\rho = \max[\hat{\varepsilon}^{1/(n_d+1)}, \tau]$.

- *In the case* $M = 0$ *(filtering differentiator* (1.29)*,* (1.30)*) the accuracy* (1.31)*,* (1.32) *holds for any* $\hat{\varepsilon}, \tau \geq 0$.
- *In the case* $M > 0$ *the accuracy holds for sufficiently small* $\hat{\varepsilon}, \tau \geq 0$*. In the case* $\hat{\varepsilon} = 0, \tau = 0$ *the convergence is in FT and exact, and is exponential to any ball of differentiation errors.*

The following is some explanation. Recall that the hybrid filtering differentiator (1.34), (1.35) turns into the filtering differentiator (1.29), (1.30) for $M = 0$ and $L = \text{const}$. It is also homogeneous in bilimit. Correspondingly in a small vicinity of the manifold $z_0 - f_0 = \ldots = z_{n_d} - f_0^{(n_d)} = 0$, $w = 0$ the error dynamics of the hybrid filtering differentiator (1.34), (1.35) corresponding to $M > 0$ and the filtering differentiator (1.29), (1.30) corresponding to $M = 0$ (asymptotically) coincide. The same happens to the discretization (1.45). This leads to the same accuracy of the both differentiators, provided ρ is small.

If ρ is large enough, the linear dynamics prevail, and the hybrid filtering differentiator effectively turns into a linear low-pass filter, whose frequency response and accuracy are determined by M. It causes the corresponding change in the accuracy asymptotics for larger $\hat{\varepsilon}$. Moreover, large τ can cause the instability of the limit linear error dynamics at infinity, correspondingly leading to the filter divergence [7, 58].

It is shown in [7] that the accuracy is not improved when additional integration steps are introduced between the actual sampling instants, or the integration makes use of the corresponding matrix exponent over each sampling interval.

1.6.2 Output feedback discretization

Consider system (1.7) of the relative degree r. Let it be closed by the feedback r-SMC (1.15) developed in Section 1.4 and exploiting the output differentiation,

$$\begin{array}{l} \dot{x} = a(t,x) + b(t,x)u(t_j), \hat{\sigma}(t_j) = \sigma(t_j, x(t_j)) + \eta(t_j), \\ u = \alpha U_r(z(t_j)),\ L \geq C + K_M \alpha \sup |U_r|,\ L > 0,\ t \in [t_j, t_{j+1}), \\ \delta_j(w,z)^T = D_{n_f, r-1}(w(t_j), z_0(t_j) - \hat{\sigma}(t_j), z(t_j), L)\tau_j. \end{array} \tag{1.47}$$

Here $\hat{\sigma} = \sigma + \eta$ represents the sampled value of σ corrupted by the noise η.

Theorem 5 *Let the sampling noise satisfy* $|\eta(t)| \leq \varepsilon_0$*, the sampling interval be bounded,* $0 < t_{j+1} - t_j \geq \tau$, $n_f \geq 0$*. Then the discrete output feedback control from* (1.47) *in FT provides for the accuracy* $|\sigma^i| \leq \gamma_i \rho^{r-i}$, $i = 0, 1, ..., r-1$*, for* $\rho = \max[(\varepsilon_0/L)^{1/(n_d+1)}, \tau]$ *and some* $\gamma_0, ..., \gamma_{r-1} > 0$.

Addition of the terms $T_{n_f, n_d}(z(t_j), \tau_j)$ in (1.47) is optional, but not required. Also this theorem formally covers the limit case $\tau = 0$ corresponding to the continuous sampling of σ in the presence of the Lebesgue-measurable noise $\eta(t)$, $|\eta(t)| \leq \varepsilon_0$. The proofs of Theorems 4, 5 are based on the accuracy estimation (1.6) of the disturbed homogeneous systems.

1.7 Filtering noises

In this section we show that the proposed differentiators and output-feedback SM controllers filter out large sampling noises, while still preserving the exactness in the absence of noises and the asymptotically optimal accuracy (1.27) in the presence of bounded noises.

1.7.1 Filtering noises in continuous time

Recall a few notions from [59].

A signal $\nu(t)$, $\nu : [0, \infty) \to \mathbb{R}$, is called *globally filterable* [59], or a *signal of the (global) filtering order* $k \geq 0$, if it is a locally integrable Lebesgue-measurable function, and there exists a globally bounded Caratheodory solution $\xi(t)$, $\xi : [0, \infty) \to \mathbb{R}$, of the equation $\xi^{(k)} = \nu$. Correspondingly $\xi^{(k-1)}(t)$ is a locally absolutely-continuous function, if $k > 0$. Naturally $\nu(t)$ is said to have the filtering order $k = 0$, if ν is essentially bounded. Any number exceeding $\sup |\xi(t)|$ is called a *kth-order (global) integral magnitude of* ν.

Assumption 1 The sampled input is of the form $f(t) = f_0(t) + \eta(t)$, where $f_0^{(n_d)}$ is a Lischitzian function, $|f_0^{(n_d+1)}(t)| \leq L$ for almost all $t > 0$ and known $L > 0$, i.e. $f_0 \in \text{Lip}_{n_d} L$. □

Assumption 2 The noise $\eta(t)$ admits an expansion of the form $\eta(t) = \eta_0(t) + \eta_1(t) + ... + \eta_{n_f}(t)$, where each η_k, $k = 0, ..., n_f$, is a signal of the global filtering order k and the kth-order integral magnitude $\varepsilon_k \geq 0$. Correspondingly, the noise components $\eta_1, ..., \eta_{n_f}$ are possibly unbounded, whereas η_0 is essentially bounded, $\operatorname{ess\,sup}_{t\geq 0} |\eta_0| \leq \varepsilon_0$. □

Introduce parameter ρ measuring the filtered intensity of the sampling noise

$$\rho = \max\left[\left(\tfrac{\varepsilon_0}{L}\right)^{\frac{1}{n_d+1}}, \left(\tfrac{\varepsilon_1}{L}\right)^{\frac{1}{n_d+2}}, ..., \left(\tfrac{\varepsilon_{n_f}}{L}\right)^{\frac{1}{n_d+n_f+1}}\right]. \tag{1.48}$$

The following two theorems appear in [37]. Recall that for $M = 0$ the hybrid filtering differentiator (1.34), (1.35) turns into the filtering one (1.29), (1.30).

Theorem 6 *Under Assumptions 1, 2 the practical stability of the hybrid filtering differentiator* (1.34)*,* (1.35) *is preserved for any ρ defined by* (1.48)*. For any ρ if $M = 0$, and for sufficiently small ρ if $M > 0$, after some FT transient the hybrid filtering differentiator* (1.34)*,* (1.35) *provides for the accuracy* (1.31)*, i.e.*

$$\begin{aligned} &|w_1| \leq \gamma_{w_1} L\rho^{n_f+n_d+1}, \\ &\left|z_i - f_0^{(i)}(t)\right| \leq \gamma_i L\rho^{n_d+1-i},\ i = 0, ..., n_d \end{aligned} \tag{1.49}$$

for some $\gamma_{w_1}, \gamma_i > 0$.

Example 3 The noise $\eta = A\cos(\omega t)$ features any global filtering order $k \geq 0$ and the integral magnitude A for $k = 0$ and $2A/\omega^k$ for $k > 0$. Theorem 6 implies that the accuracy estimation (1.49), (1.48) holds for each possible expansion $\eta = \eta_0 + ... + \eta_{n_f}$. In particular, $\eta = \eta_{n_f}$ corresponds to $\rho = (A/L)^{1/(n_d+n_f+1)}\omega^{-n_f/(n_d+n_f+1)}$.

Note that for sufficiently large n_f the resulting noise-intensity parameter ρ of the harmonic signal approaches the number $1/\omega$ and does not depend on A. On the other hand, the theorem provides an upper estimation valid for any possible expansion of η into a sum of filterable signals η_k. For sufficiently small A another estimation $\rho = (A/L)^{1/(n_d+1)}$ corresponding to $\eta = \eta_0$ provides a better estimation and leads to the asymptotically optimal asymptotics (1.27). Indeed, for sufficiently small A one gets $f \in \mathrm{Lip}_{n_d} L$ and the differentiator is to exactly differentiate the noise.

The *unbounded* signals $\eta = A\frac{d^k}{dt^k}\lfloor\cos(\omega t)\rceil^{\beta}$, $\beta \in (k-1, k)$, $k = 1, 2, ...,$ feature the filtering order k and the integral magnitude A. □

Consider now the output-feedback closed-loop system

$$\begin{aligned} &\dot{x} = a(t,x) + b(t,x)u, \hat{\sigma} = \sigma(t,x) + \eta(t), \\ &u = \alpha U_r(z),\ L \geq C + K_M\alpha \sup|U_r|,\ L > 0, \\ &(\dot{w}, \dot{z})^T = D_{n_f,r-1}(w, z_0 - \hat{\sigma}, L). \end{aligned} \tag{1.50}$$

The following theorem follows [37].

Theorem 7 *Under Assumption 2 after some FT transient closed system* (1.50) *converges into the region* $|\sigma^i| \le \gamma_i \rho^{r-i}$*,* $i = 0, 1, ..., r-1$*, for some constant* $\gamma_i > 0$*. The result holds for any* ρ *provided by* (1.48) *if* $M = 0$*, and for sufficiently small* ρ *if* $M > 0$*. System preserves its practical stability for any* ρ*.*

The next notion extends the corresponding definition from [59] and is employed to demonstrate that the conditions on the noise are actually of the local nature.

A locally integrable Lebesgue-measurable function $\nu(t)$, $\nu : [0,\infty) \to \mathbb{R}$, is called *locally* T*-filterable* signal of the filtering order $k > 0$ and the *integral magnitudes* $a_0, a_1, ..., a_{k-1} \ge 0$, if there exists an infinite sequence $t_0, t_1, ...,$ $t_0 \ge 0$, $t_{j+1} - t_j \ge T > 0, j = 0, 1, ...,$ such that for each j there exists a Caratheodory solution $\xi(t)$, $t \in [t_j, t_{j+1}]$, of the equation $\xi^{(k)}(t) = \nu(t)$ which satisfies $|\xi^{(l)}(t)| \le a_l$ for $l = 0, 1, ..., k-1$. The number a_l is called the *local* $(k-l)$*th-order integral magnitude of* ν. Signals of local filtering order 0 are trivially defined as uniformly essentially bounded Lebesgue-measurable signals of the magnitude a_0, $\operatorname{ess\,sup}_{t\ge 0} |\nu(t)| \le a_0$.

In particular, locally filterable noises can be concatenated producing new locally filterable noises. The following lemma [59] shows that filtering differentiators can be applied when the noises are only locally filterable.

Lemma 1 *Any signal* $\nu(t)$ *of the* ***local*** T*-filtering order* $k \ge 0$ *can be represented as* $\nu = \eta_0 + \eta_1 + \eta_k$*, where* η_0, η_1, η_k *are signals of the (****global****) filtering orders* $0, 1, k$ *respectively. Their magnitudes continuously depend on* $\vec{a}_{k-1}$ *and* T*.*

In particular, in the important case $k = 1$ *get* $\nu = \eta_0 + \eta_1$*, where* $|\eta_0| \le a_0/T$*, and the first-order integral magnitude of* η_1 *is* $2a_0$*. In the general case* $k > 1$ *fix any number* $\hat\rho_0 > 0$*. Then, provided* $\hat\rho \le \hat\rho_0$ *holds for* $\hat\rho = \max[a_0^{1/k}, a_1^{1/(k-1)}, ..., a_{k-1}]$*, the integral magnitudes of the signals* η_0, η_1, η_k *are calculated as* $\gamma_0 \hat\rho/T$*,* $\gamma_1 \hat\rho$*,* $\gamma_k \hat\rho^k$ *respectively, where the constants* $\gamma_0, \gamma_1, \gamma_k > 0$ *only depend on* k *and* $\hat\rho_0$*.*

1.7.2 Filtering noises in discrete time

Once more, let the sampling take place at the times $t_0, t_1, \ldots, t_0 = 0, t_{j+1} - t_j = \tau_j \le \tau$. Due to the Nyquist-Shannon sampling rate principle noises small in average under one sequence $\{t_j\}$ can be large under another. Therefore, the admissible sampling-time sequences are to exist for any $\tau > 0$. Correspondingly, the set of such sequences is infinite.

A discretely sampled signal $\nu : \mathbb{R}_+ \to \mathbb{R}$ is said to be of the *global sampling filtering order* $k \ge 0$ and the *global kth order integral sampling magnitude* $a \ge 0$ if for each admissible sequence t_j there exists a discrete vector signal $\xi(t_j) = (\xi_0(t_j), ..., \xi_k(t_j))^T \in \mathbb{R}^{k+1}, j = 0, 1, ...,$ satisfying the relations $\delta_j \xi_i = \xi_{i+1}(t_j)\tau_j$, $i = 0, 1, ..., k-1$, $\xi_k(t_j) = \nu(t_j)$, $|\xi_0(t_j)| \le a$.

Theorems similar to Theorems 6, 7 hold also here [37, 59].

Assumption 3 The noise $\eta(t_j)$ admits an expansion of the form $\eta(t_j) = \eta_0(t_j) + \eta_1(t_j) + ... + \eta_{n_f}(t_j)$, where each η_k, $k = 0, ..., n_f$, is a signal of the global sampling filtering order k and the kth-order sampling integral magnitude $\varepsilon_k \ge 0$. □

Introduce parameter ρ measuring the discrete filtered sampling noise intensity,

$$\rho = \max\left[\tau, \left(\frac{\varepsilon_0}{L}\right)^{\frac{1}{n_d+1}}, \left(\frac{\varepsilon_1}{L}\right)^{\frac{1}{n_d+2}}, ..., \left(\frac{\varepsilon_{n_f}}{L}\right)^{\frac{1}{n_d+n_f+1}}\right]. \tag{1.51}$$

Theorem 8 *Under Assumptions 1, 3 after some FT transient the hybrid filtering differentiator* (1.45)*,* (1.46) *provides for the accuracy* (1.49) *for ρ, τ small enough if $M > 0$, or for any ρ if $M = 0$. The practical stability of the filter is preserved for any ρ if $M = 0$ and for sufficiently small τ if $M > 0$.*

Theorem 9 *Under Assumption 3 the closed system* (1.47) *in FT stabilizes in the region $|\sigma^i| \leq \gamma_i \rho^{r-i}$, $\gamma_i > 0$, $i = 0, 1, ..., r-1$, for ρ defined by* (1.51)*. It holds for any $\rho \geq 0$ if $M = 0$, and for sufficiently small ρ, τ if $M > 0$. The system practical stability is preserved for any ρ if $M = 0$ and for sufficiently small τ if $M > 0$.*

The following notion extends the similar one from [59].

A discretely sampled signal $\nu(t_j)$ is said to be *locally T-filterable of the local sampling filtering order* $k > 0$ and the *integral magnitudes* $a_0, a_1, ..., a_{k-1} \geq 0$, if there exists an infinite sequence $\hat{t}_0, \hat{t}_1, ..., \hat{t}_0 \geq 0, \hat{t}_{l+1} - \hat{t}_l \geq T > 0, l = 0, 1, ...,$ such that for any sufficiently small τ, admissible sequence $\{t_j\}$, and any $l \geq 0$ there exists a discrete vector signal $\xi(t_j) = (\xi_0(t_j), ..., \xi_k(t_j))^T \in \mathbb{R}^{k+1}$, $j = j_0, j_0 + 1, ..., j_1$, $t_{j_0} \in [\hat{t}_l, \hat{t}_l + \tau)$, $t_{j_1} \in (\hat{t}_{l+1} - \tau, \hat{t}_{l+1}]$, which satisfies the relations

$$\begin{aligned} &\delta_j \xi_i = \xi_{i+1}(t_j)\tau_j, \ i = 0, 1, ..., k-1, \\ &\xi_k(t_j) = \nu(t_j), \ |\xi_i(t_j)| \leq a_i. \end{aligned} \tag{1.52}$$

Numbers a_i are called the *local $(k-i)$th-order sampling integral magnitudes of ν*. Signals of local sampling filtering order 0 by definition are just bounded signals of the magnitude a_0.

Similarly to the continuous-time case, one can concatenate locally filterable signals. The following lemma [59] similar to Lemma 1 justifies application of Theorems 8, 9 in the case of locally filterable sampled noises.

Lemma 2 *Let all admissible sampling time sequences satisfy the condition* $\sup \tau_j \leq c_\tau \inf \tau_j$ *for some $c_\tau > 0$. Then any discretely sampled signal $\nu(t_j)$ of the* ***local*** *sampling T-filtering order $k \geq 0$ can be represented as $\nu = \eta_0 + \eta_1 + \eta_k$, where η_0, η_1, η_k are signals of the (global) sampling filtering orders $0, 1, k$.*

In particular, if $k = 1$ get $\nu = \eta_0 + \eta_1$, where $|\eta_0| \leq a_0/T$, and the first-order integral sampling magnitude of η_1 is $2a_0$. If $k > 1$ fix any number $\rho_0 > 0$. Then, provided $\rho = \max[a_0^{1/k}, a_1^{1/(k-1)}, ..., a_{k-1}] \leq \rho_0$ the sampling integral magnitudes of the signals η_0, η_1, η_k are calculated as $\gamma_0 \rho/T$, $\gamma_1 \rho$, $\gamma_k \rho^k$ respectively, where the constants $\gamma_0, \gamma_1, \gamma_k > 0$ only depend on k and ρ_0.

It is easy to prove that any *bounded continuous* periodic signal featuring a local T-filtering order is transformed into a discrete signal of the same sampling filtering order, provided $\sup \tau_j \leq c_\tau \inf \tau_j$ holds for some $c_\tau > 0$. It follows from the convergence of the Euler approximations to the unique solutions of DEs [31]. Also the smaller τ the closer are the integral sampling magnitudes to those of the original continuous-time signal.

Any *bounded* periodic noise of a global filtering order is trivially of the same local filtering order. Correspondingly Lemma 2, establishes its effective suppression by a filtering or a hybrid filtering discrete differentiator.

It is *wrong* to claim that sampling any globally filterable signal of the order k produces a discrete signal of the same global sampling filtering order k. Indeed, a multiple numeric integral of the unbounded signal from Example 3 can become very large for some concrete sampling sequence t_j and even cause computer overflow. The issue is resolved by introducing a saturation of the sampled periodic unbounded signal, even if a very high saturation level is taken.

1.8 Numeric differentiation

1.8.1 Numeric homogeneous differentiation

Consider the noisy input signal

$$f(t) = f_0(t) + \eta(t),\; f_0(t) = 0.5\cos(t) + 0.9\sin(0.5t + \log(t+1)). \tag{1.53}$$

Obviously, for each $k > 0$ the inequality $|f_0^{(k)}(t)| \leq 1$ holds starting from some moment. Let the noise η be composed of three components

$$\begin{array}{l} \eta(t) = \eta_1(t) + \eta_2(t) + \eta_3(t), \\ \eta_1(t) \in N(0, 0.2^2), \\ \eta_2(t) = 10^7\cos(10^8 t), \\ \eta_3(t) = 0.1\cos(10^4 t)\left\lfloor\sin(10^4 t)\right\rceil^{-\frac{1}{2}} = 2\cdot 10^{-5}\frac{d}{dt}\left\lfloor\sin(10^4 t)\right\rceil^{\frac{1}{2}}, \end{array} \tag{1.54}$$

where η_1 is a random Gaussian signal of the standard deviation 0.2, η_2 is a large high-frequency harmonic signal, and η_3 is an unbounded signal of the filtering order 1 and the integral magnitude $2\cdot 10^{-5}$ (Example 3). The noise components are presented in Fig. 1.1.

Apply the discrete filtering differentiator (1.45) of the differentiation order $n_d = 2$ and the filtering order $n_f = 8$ with the parameters (1.37), $L = 1$, $M = 0$, and the constant sampling step $\tau_j = \tau = 10^{-6}$. The simulation is performed over the time interval $[0, 25]$.

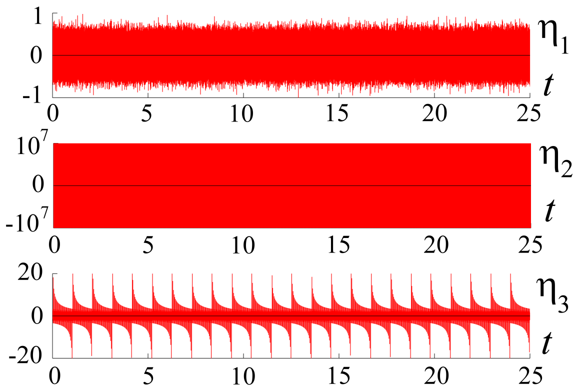

Fig. 1.1 Graphs of the noise components (1.54). η_1 is a Gaussian noise, η_2 is a large high-frequency harmonic noise, and η_3 is an unbounded noise of the filtering order 1.

Performance of the discrete filtering differentiator in the absence of noise is presented in Fig. 1.2. Practically exact convergence is demonstrated. The resulting accuracy is presented by the component-wise inequality

$$(|w_1|, |w_2|, |w_3|, |w_4|, |w_5|, |w_6|, |w_7|, |w_8|, |z_0 - f_0|, |z_1 - \dot{f}_0|, |z_2 - \ddot{f}_0|) \leq (1.6 \cdot 10^{-54}, 2.7 \cdot 10^{-48}, 2.6 \cdot 10^{-42}, 1.3 \cdot 10^{-36}, 4.0 \cdot 10^{-31}, 7.0 \cdot 10^{-26}, 6.2 \cdot 10^{-21}, 2.7 \cdot 10^{-16}, 4.9 \cdot 10^{-12}, 4.8 \cdot 10^{-5}, 1.8 \cdot 10^{-4}). \quad (1.55)$$

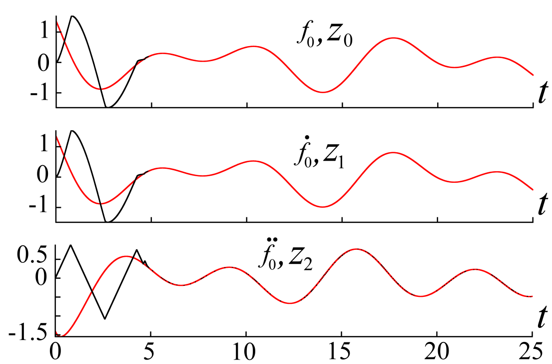

Fig. 1.2 Performance of the discrete filtering differentiator (1.45) with $n_d = 2$, $n_f = 8$, $L = 1$, $M = 0$, $\tau = 10^{-6}$ in the absence of noises, $\eta = 0$, for the input (1.53). Estimations of $f_0, \dot{f}_0, \ddot{f}_0$ are shown.

Performance of the differentiator separately for each noise component is demonstrated in Figs. 1.3, 1.4, 1.5. The accuracy obtained for the Gaussian noise $\eta = \eta_1$

is

$$(|w_1|, |w_2|, |w_3|, |w_4|, |w_5|, |w_6|, |w_7|, |w_8|, |z_0 - f_0|, |z_1 - \dot{f}_0|, |z_2 - \ddot{f}_0|) \leq (1.2 \cdot 10^{-23}, 3.7 \cdot 10^{-20}, 6.8 \cdot 10^{-17}, 6.4 \cdot 10^{-14}, 3.4 \cdot 10^{-11}, 1.1 \cdot 10^{-8}, 1.6 \cdot 10^{-6}, 1.3 \cdot 10^{-4}, 2.6 \cdot 10^{-3}, 2.9 \cdot 10^{-2}, 1.7 \cdot 10^{-1}). \quad (1.56)$$

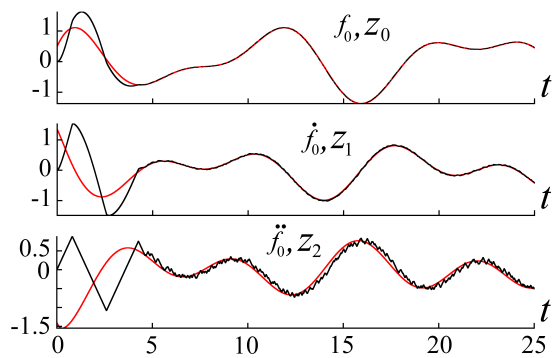

Fig. 1.3 Performance of the discrete filtering differentiator with $n_d = 2$, $n_f = 8$, $L = 1$, $\tau = 10^{-6}$ for the input (1.53) corrupted by the Gaussian sampling noise $\eta = \eta_1 \in N(0, 0.2^2)$. Estimation of $f_0, \dot{f}_0, \ddot{f}_0$ is shown.

It has been shown in a qualitative way [52] that random non-correlated sampled noises of the same distribution feature the first filtering order, and can be practically canceled for sufficiently small sampling constant step. In other words the integral magnitude of the noise tends to zero as the sampling rate tends to infinity, but this convergence is very slow. Increasing the filtering order n_f does not significantly affect the differentiator performance in that case.

Contrary to the Gaussian noises harmonic noises of high frequency are very well filtered (Fig. 1.4). The higher the filtering order the better is the result. It is shown in Example 3 that the influence of small and large harmonic noises of the same frequency are almost the same for large n_f. In that case the noise-intensity parameter ρ approaches $1/\omega$ where ω is the noise frequency, and $|z_i - f_0^{(i)}| \leq \gamma_i L^{\frac{i}{n_d+1}} \rho^{\frac{n_d+1-i}{n_d+1}}$. Thus from some moment further increasing n_f does not provide an accuracy improvement. The accuracy obtained for the harmonic noise η_2 is

$$(|w_1|, |w_2|, |w_3|, |w_4|, |w_5|, |w_6|, |w_7|, |w_8|, |z_0 - f_0|, |z_1 - \dot{f}_0|, |z_2 - \ddot{f}_0|) \leq (1.0 \cdot 10^{-25}, 4.9 \cdot 10^{-22}, 1.4 \cdot 10^{-18}, 2.0 \cdot 10^{-15}, 1.6 \cdot 10^{-12}, 8.6 \cdot 10^{-10}, 3.7 \cdot 10^{-5}, 19.1, 4.0 \cdot 10^{-4}, 7.9 \cdot 10^{-3}, 8.3 \cdot 10^{-2}). \quad (1.57)$$

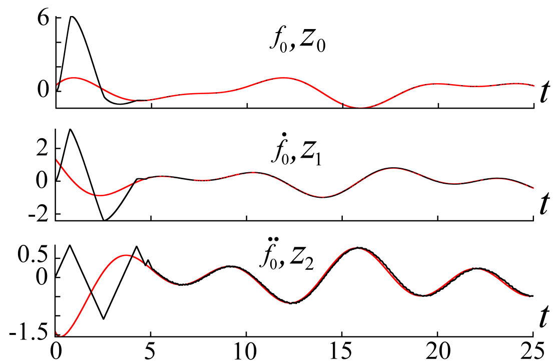

Fig. 1.4 The discrete filtering differentiator with $n_d = 2$, $n_f = 8$, $L = 1$, $\tau = 10^{-6}$ with the input (1.53) is almost insensitive to the noise $\eta = \eta_2 = 10^7 \cos(10^8 t)$ featuring both extremely large magnitude and extremely high frequency. Estimation of $f_0, \dot{f}_0, \ddot{f}_0$ is shown.

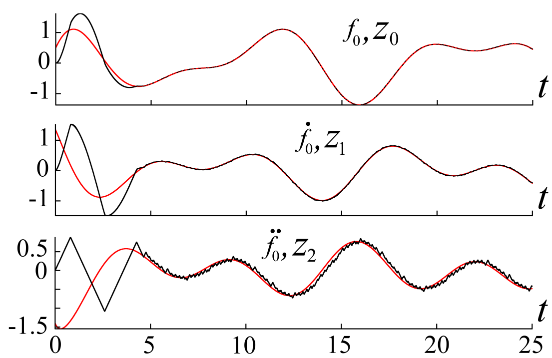

Fig. 1.5 Performance of the discrete filtering differentiator with $n_d = 2$, $n_f = 8$, $L = 1$, $\tau = 10^{-6}$ for the input (1.53) corrupted by the unbounded noise $\eta = \eta_3$ of the filtering order 1. Estimation of $f_0, \dot{f}_0, \ddot{f}_0$ is shown.

The considered unbounded noise has the filtering order 1 (Example 3, Fig. 1.5). It means that increasing $n_f > 1$ does not improve accuracy, which is determined by the noise average value. Noises of the type η_1 and η_3 are most difficult for the filtering differentiator. The accuracy obtained for the unbounded noise $\eta = \eta_3$ is

$$\begin{aligned}
&(|w_1|, |w_2|, |w_3|, |w_4|, |w_5|, |w_6|, |w_7|, |w_8|, |z_0 - f_0|, |z_1 - \dot{f}_0|, |z_2 - \ddot{f}_0|) \leq \\
&\quad (7.3 \cdot 10^{-24}, 2.3 \cdot 10^{-20}, 4.4 \cdot 10^{-17}, 4.4 \cdot 10^{-14}, 2.5 \cdot 10^{-11}, 8.0 \cdot 10^{-9}, \\
&\qquad 1.3 \cdot 10^{-6}, 1.2 \cdot 10^{-4}, 2.3 \cdot 10^{-3}, 2.3 \cdot 10^{-2}, 1.6 \cdot 10^{-1}). \qquad (1.58)
\end{aligned}$$

Note that the high frequencies of η_2, η_3 form a special challenge for the differentiator. In fact, the authors cannot rigorously explain, how the differentiator removes

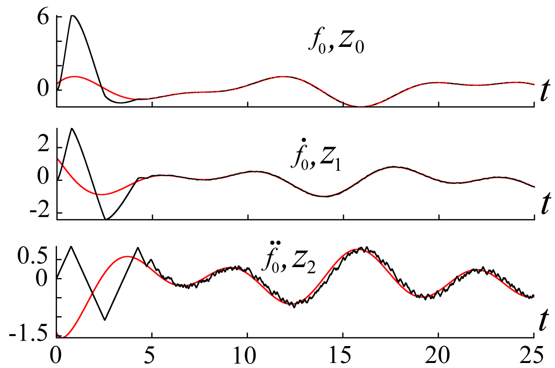

Fig. 1.6 Performance of the discrete filtering differentiator, $n_d = 2$, $n_f = 8$, $L = 1$, $\tau = 10^{-6}$, for the input (1.53) and the combined noise (1.54). Estimation of f_0, $\dot{f}_0$, $\ddot{f}_0$ is shown.

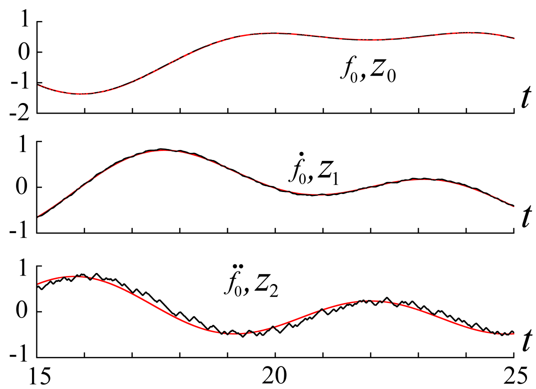

Fig. 1.7 Performance of the discrete filtering differentiator, $n_d = 2$, $n_f = 8$, $L = 1$, $\tau = 10^{-6}$, for the input (1.53) and the combined noise (1.54). A zoom of the approximation graphs z_0, f_0, z_1, $\dot{f}_0$ and z_2, $\ddot{f}_0$ is shown.

a noise of a period which is at least 16 times less than the sampling step (also see the simulation in Sections 1.9.2.2, 1.9.3.1).

The performance of the filtering differentiator for the input (1.53) in the presence of the combined noise (1.54) is presented in Figs. 1.6, 1.7. The resulting accuracy for $t \in [20, 25]$ is provided by the component-wise inequality

$$(|w_1|, |w_2|, |w_3|, |w_4|, |w_5|, |w_6|, |w_7|, |w_8|, |z_0 - f_0|, |z_1 - \dot{f}_0|, |z_2 - \ddot{f}_0|) \leq (5 \cdot 10^{-23}, 1.4 \cdot 10^{-19}, 2.2 \cdot 10^{-16}, 1.8 \cdot 10^{-13}, 8.6 \cdot 10^{-11}, 2.3 \cdot 10^{-8}, 3.9 \cdot 10^{-5}, 19, 0.003, 0.029, 0.167). \quad (1.59)$$

Note that w_8 has seemingly absorbed the main part of the noise.

Compare the accuracies (1.56), (1.57), (1.58) obtained separately for each noise component with the accuracy (1.59) obtained for the composite noise (1.54). One clearly sees that there is no superposition principle. The overal maximal errors are closer to the maximal errors obtained for each noise component than to their sum.

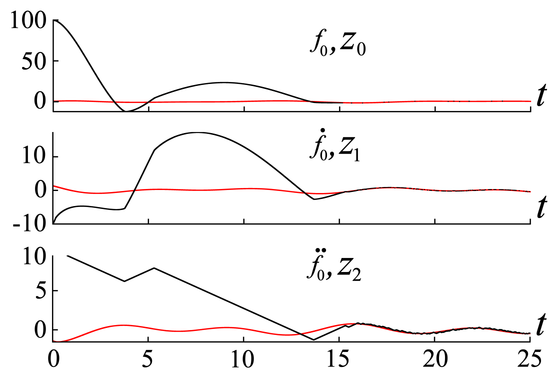

Fig. 1.8 Performance of the discrete filtering differentiator with $n_d = 2$, $n_f = 8$, $L = 1$, $\tau = 10^{-6}$ for the input (1.53) and the combined noise (1.54). The initial state is $z(0) = (100, -10, 10)$. Estimation of $f_0, \dot{f}_0, \ddot{f}_0$ is shown.

1.8.2 Numeric hybrid differentiation

Filtering differentiators feature slow convergence rate from significant initial errors. Hybrid filtering differentiators provide practically the same accuracy for the considered noises, but feature much faster convergence.

Consider the same noisy input but with the non-zero differentiator initial state $z_0(0) = 100, z_1(0) = -10, z_2(0) = 10$. Then the above filtering differentiator, corresponding to $M = 0$, has the convergence time of about 15 time units, whereas the filtering hybrid differentiator with $M = 1$ demonstrates the convergence time of about 5 units. The larger the initial errors the larger the difference. For really large

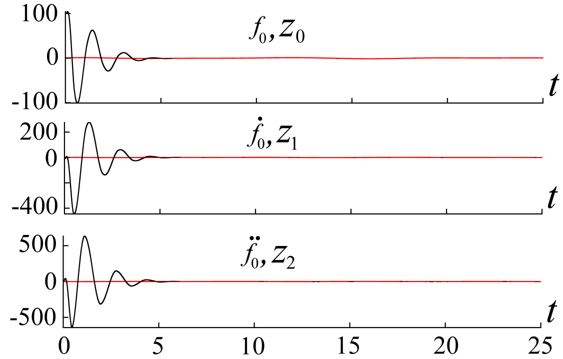

Fig. 1.9 Performance of the discrete filtering *hybrid* differentiator with $n_d = 2$, $n_f = 8$, $L = 1$, $M = 1$, $\tau = 10^{-6}$ for the input (1.53) and the combined noise (1.54). The initial state is $z(0) = (100, -10, 10)$. The convergence is significantly faster compared with the filtering differentiator (the case $M = 0$). Estimation of $f_0, \dot{f}_0, \ddot{f}_0$ is shown.

initial errors implementation of the homogeneous SM-based differentiators becomes impossible (see the simulation in Section 1.9.3.1).

1.8.3 Comparison with the Kalman filter

Compare the performance of the standard Kalman filter (KF) and the filtering differentiator (FD). Once more consider the input signal (1.53)

$$f(t) = f_0(t) + \eta(t), \;\; f_0(t) = 0.5\cos(t) + 0.9\sin(0.5t + \log(t+1)), \tag{1.60}$$

where η is a noise. As mentioned previously for each k from some moment $|f_0^{(k)}| \leq 1$ holds.

The filtering differentiator is once more of the differentiation order $n_d = 2$ and the filtering order $n_f = 8$, $L = 1$, $\tau = 10^{-6}$. The Kalman prediction and innovation equations are

$$\begin{aligned} \hat{x}_{j+1} &= \Phi_j \hat{x}_j, \\ y(t_j) &= f(t_j) - H\hat{x}_j, \end{aligned} \tag{1.61}$$

where $\hat{x}_j$ and $y(t_j)$ respectively are the estimation of $(f_0, \dot{f}_0, \ddot{f}_0)^T$ and the Kalman innovation. The state transition and the measurement models are

$$\Phi_j = \begin{bmatrix} 1 & \tau & \frac{\tau^2}{2} \\ 0 & 1 & \tau \\ 0 & 0 & 1 \end{bmatrix}, H = \begin{bmatrix} 1 & 0 & 0 \end{bmatrix} \tag{1.62}$$

respectively. The covariance matrix of $\hat{x}_j$ is propagated with the noise covariance matrix

$$Q_j = \begin{bmatrix} 0 & 0 & 0 \\ 0 & 0 & 0 \\ 0 & 0 & \tau \end{bmatrix}. \tag{1.63}$$

The Kalman update is applied with an appropriate scalar measurement-noise covariance matrix $R \in \mathbb{R}$ to be specified further.

First consider the Gaussian noise $\eta(t) \in N(0, 0.2^2)$ of the standard deviation 0.2. Correspondingly, $R = 0.2^2$ is taken. Performance of both filters is presented in Figs. 1.10, 1.11. The resulting accuracy for $t \in [8, 10]$ is provided by the component-wise inequality

$$\begin{array}{l} KF: \ (|z_0 - f_0|, |z_1 - \dot{f}_0|, |z_2 - \ddot{f}_0|) \leq (0.003, 0.046, 0.395), \\ FD: \ (|z_0 - f_0|, |z_1 - \dot{f}_0|, |z_2 - \ddot{f}_0|) \leq (0.00278, 0.02364, 0.113). \end{array} \tag{1.64}$$

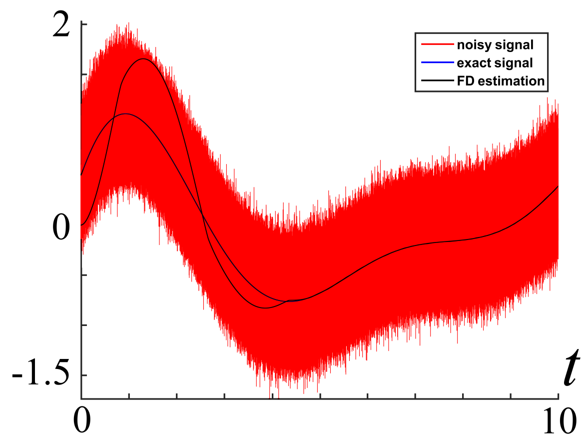

Fig. 1.10 Performance of numeric filtering differentiator with $n_d = 2, n_f = 8, L = 1, \tau = 10^{-6}$ for the input (1.60) corrupted by the Gaussian noise $\eta(t) \in N(0, 0.2^2)$. Estimation of f_0 is shown.

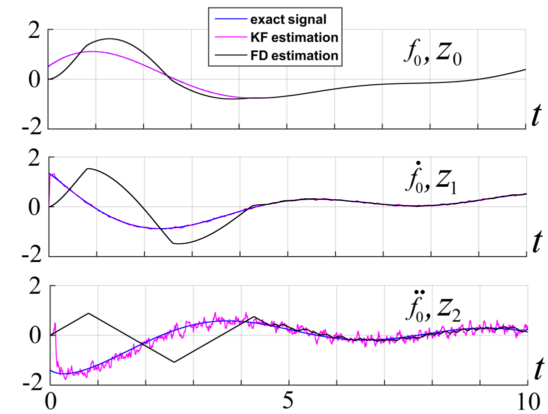

Fig. 1.11 Performance of Kalman filter (KF) and the filtering differentiator (FD) with $n_d = 2$, $n_f = 8$, $L = 1$, $\tau = 10^{-6}$ for the input (1.60) and the Gaussian noise $\eta(t) \in N(0, 0.2^2)$. Estimation of $f_0, \dot{f}_0, \ddot{f}_0$ is shown.

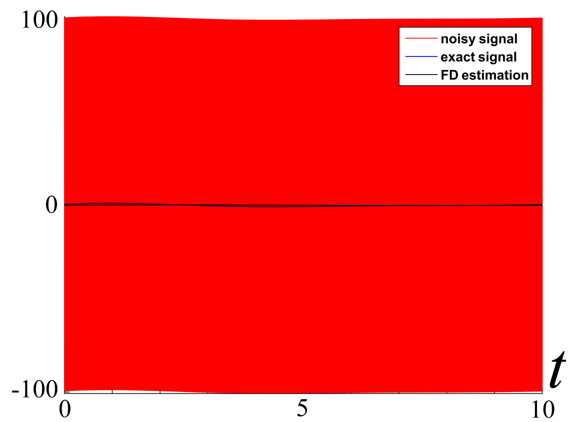

Fig. 1.12 Performance of the FD with $n_d = 2$, $n_f = 8$, $L = 1$, $\tau = 10^{-6}$ for the input (1.60) corrupted by the harmonic noise $\eta(t) = 100\cos(10^8 t)$. Estimation of f_0 is shown.

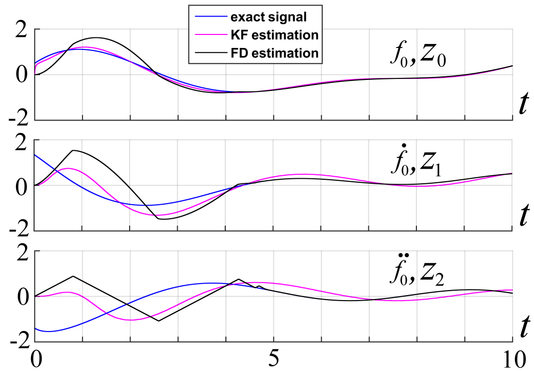

Fig. 1.13 Performance of the KF with $R = 100^2$ and the FD with $n_d = 2$, $n_f = 8$, $L = 1$, $\tau = 10^{-6}$ in the presence of the harmonic noise $\eta(t) = 100\cos(10^8 t)$. Estimation of $f_0, \dot{f}_0, \ddot{f}_0$ is shown.

Consider a large high-frequency harmonic noise $\eta(t) = 100\cos(10^8 t)$. In this case two different measurement covariance matrices are considered: $R = 0.2^2$ (as previously) and $R = 100^2$ corresponding to the noise magnitude. Performance of both filters is presented in Figs. 1.12, 1.13. The corresponding accuracies for $t \in [8, 10]$ are as follows:

$$\begin{array}{ll} KF(R = 0.2^2): & (|z_0 - f_0|, |z_1 - \dot{f}_0|, |z_2 - \ddot{f}_0|) \leq (0.0065, 0.1135, 0.99), \\ KF(R = 100^2): & (|z_0 - f_0|, |z_1 - \dot{f}_0|, |z_2 - \ddot{f}_0|) \leq (0.03, 0.1323, 0.2754), \\ FD: & (|z_0 - f_0|, |z_1 - \dot{f}_0|, |z_2 - \ddot{f}_0|) \leq (3.9 \cdot 10^{-5}, 0.003, 0.029). \end{array} \tag{1.65}$$

Note that in order to provide for the good performance of the Kalman filter one needs to adjust the covariance parameter R using some knowledge on the sampling noise. Contrary to this, we do not change the parameters of the filtering differentiator, and do not need to know whether any noise is present.

1.9 Output-feedback control simulation

In this section we demonstrate the efficiency, application simplicity and robustness of the developed SM controllers and observers. Two different academic examples are presented. The first one is a disturbed integrator chain of the relative degree 3, whereas the second one is a slightly modified one-link robot inspired by the classical example [40] of the relative degree 4.

1.9.1 Homogeneous SM control development

Let the relative degree be $r \in \mathbb{N}$. Then the r-SM homogeneity weights are $\deg \sigma = r, \deg \dot{\sigma} = r-1, ..., \deg \sigma^{(k)} = r-k$, $0 \le k \le r$. Choose a homogeneous norm valid for $k < r$:

$$||\vec{\sigma}_k||_{h\infty} = ||(\sigma, ..., \sigma^{(k)})||_{h\infty} = \max[|\sigma|^{\frac{1}{r}}, ..., |\sigma^{(k)}|^{\frac{1}{r-k}}].$$

Any other homogeneous norm can be chosen here. Also recall that $\vec{\sigma}_{r-1}$ constitute the r-SM homogeneous coordinates.

1.9.1.1 4-SMC development

First develop a universal 4-SMC. The homogeneity weights of the sliding variables are $\deg \sigma = 4$, $\deg \dot{\sigma} = 3$, $\deg \ddot{\sigma} = 2$, $\deg \dddot{\sigma} = 1$; $\deg t = 1$.

According to Section 1.4.1 start with the 1st-order homogeneous FTS DE

$$\dot{\sigma} + \beta_0 \lfloor \sigma \rceil^{3/4} = 0, \ \beta_0 > 0.$$

Any value $\beta_0 > 0$ is valid. Choose and substitute $\beta_0 = 1$.

The second order DE has already infinitely many options (Section 1.4.1). Choose

$$\ddot{\sigma} + \beta_1 ||\vec{\sigma}_1||_{h\infty}^{\frac{1}{2}} \left\lfloor \dot{\sigma} + \lfloor \sigma \rceil^{\frac{3}{4}} \right\rceil^{\frac{1}{2}} = 0, \ \beta_1 > 0.$$

According to Theorem 3 it is FTS for sufficiently large $\beta_1 > 0$. Simulation shows that $\beta_1 = 1$ fits.

The 3rd-order FTS DE is chosen in the form

$$\dddot{\sigma} + \beta_2 \left\lfloor \ddot{\sigma} + ||\vec{\sigma}_1||_{h\infty}^{\frac{1}{2}} \left\lfloor \dot{\sigma} + \lfloor \sigma \rceil^{\frac{3}{4}} \right\rceil^{\frac{1}{2}} \right\rceil^{\frac{1}{2}} = 0.$$

Simulation shows that $\beta_2 = 5$ provides for the FT stability.

At the last step choose the 4-SM QC control

$$u(\vec{\sigma}_3) = -\alpha ||\vec{\sigma}_3||_{h\infty}^{-\frac{1}{2}} \left\lfloor \dddot{\sigma} + 5 \left\lfloor \ddot{\sigma} + ||\vec{\sigma}_1||_{h\infty}^{\frac{1}{2}} \left\lfloor \dot{\sigma} + \lfloor \sigma \rceil^{\frac{3}{4}} \right\rceil^{\frac{1}{2}} \right\rceil^{\frac{1}{2}} \right\rceil^{\frac{1}{2}}, \qquad (1.66)$$

where the free parameter α defines the control magnitude. Obviously, $\deg u = 0$.

When applied in the output feedback the differentiator outputs z_i are to be substituted for $\sigma^{(i)}$, $i = 0, 1, 2, 3$.

1.9.1.2 3-SMC development

Development of a universal 3-SM controller is even simpler. The homogeneity weights of the sliding variables are $\deg\sigma = 3$, $\deg\dot\sigma = 2$, $\deg\ddot\sigma = 1$; $\deg t = 1$.

Once more start with the simplest 1st-order homogeneous FTS DE

$$\dot\sigma + \beta_0\lfloor\sigma\rceil^{2/3} = 0, \beta_0 = 1.$$

The second order FTS DE is similarly chosen as

$$\ddot\sigma + \beta_1\left\lfloor\dot\sigma + \lfloor\sigma\rceil^{\frac{2}{3}}\right\rceil^{\frac{1}{2}} = 0,\ \beta_1 > 0.$$

Once more the simulation shows that $\beta_1 \geq 1$ suffices. Choose $\beta_1 = 2$.

Now the 3-SM controller is chosen as

$$u(\vec\sigma_2) = -\alpha||\vec\sigma_2||_{h\infty}^{-\frac{1}{2}}\left\lfloor\ddot\sigma + 2\left\lfloor\dot\sigma + \lfloor\sigma\rceil^{\frac{2}{3}}\right\rceil^{\frac{1}{2}}\right\rceil^{\frac{1}{2}}. \tag{1.67}$$

It is easy to see the general form of r-SM controllers incorporating controllers (1.67) and (1.66) for $r = 3$ and $r = 4$ respectively.

1.9.1.3 Output-feedback control: choice of initial observer state

In the case when only the tracking error σ is available, an observer is to provide for the estimations of $\vec\sigma_{r-1}$. However, observer application requires assignment of its initial values.

One of the ways is to choose a FxT stable observer/differentiator like [3, 21]. Such differentiator is very sensitive to sampling noises and intervals, especially to the large sampling noises we consider, and can simply diverge [54].

Another solution proposed in the past by the authors suggests approximate calculation of the initial derivative values. For this end one uses finite differences over r sampling intervals of a reasonable length. The calculation can be repeated and some average values can be taken for larger noises. That approach leads to the immediate differentiator convergence, if the noises are small. Unfortunately, the initial error can happen to be very large in the presence of significant noises.

Homogeneous differentiators [46, 59] are known to slowly converge from large initial errors (see Section 1.9.3). In the sequel we demonstrate that the hybrid (bi-homogeneous) filtering differentiators solve this problem converging fast even from large initial errors.

1.9.2 Output-feedback control of the integrator chain

Consider the disturbed third-order integrator chain

$$\begin{aligned} &\dddot{x} = \cos(x^2 + \ddot{x} + 100t + 1) + \tfrac{3+2\cos^2(1000t)}{1+\cos^2(1000t)} u, \ y = x, \\ &y_c(t) = \cos(0.5t) + 0.6\sin t, \end{aligned} \quad (1.68)$$

where y is the output of the system, and the signal $y_c(t)$ is to be tracked. The tracking error is correspondingly defined as $\sigma_y = y - y_c$. The relative degree of system (1.68) is 3.

It is easy to see that the tracking error σ_y satisfies

$$\dddot{\sigma}_y = h_y(t, x, \dot{x}, \ddot{x}) + g_y(t, x, \dot{x}, \ddot{x})u, \ |h_y| \leq 2, \ g_y \in [2, 3]. \quad (1.69)$$

Therefore, each its solution satisfies the DI

$$\dddot{\sigma}_y \in [-2, 2] + [2, 3]u. \quad (1.70)$$

Apply control (1.67) for $\alpha = 5$,

$$u = -5 \cdot ||\vec{\sigma}_{y2}||_{h\infty}^{-\frac{1}{2}} \left\lfloor \ddot{\sigma}_y + 2 \cdot \left\lfloor \dot{\sigma}_y + \lfloor \sigma_y \rceil^{\frac{2}{3}} \right\rceil^{\frac{1}{2}} \right\rceil^{\frac{1}{2}}. \quad (1.71)$$

The Euler integration method is applied with the integration step $\tau = 10^{-6}$ and the initial conditions $(x(0), \dot{x}(0), \ddot{x}(0)) = (50, -50, 50)$.

1.9.2.1 3-SM control with exact measurements

First assume that all derivatives of σ be available in real time. The corresponding performance of the system is presented in Figs. 1.14-1.16.

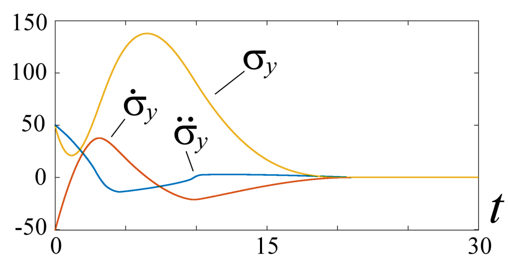

Fig. 1.14 Tracking error $\sigma_y = y - y_c$ and its derivatives $\dot{\sigma}_y, \ddot{\sigma}_y$ vs time in the case of the 3-SM Control (1.71) with full exact measurements.

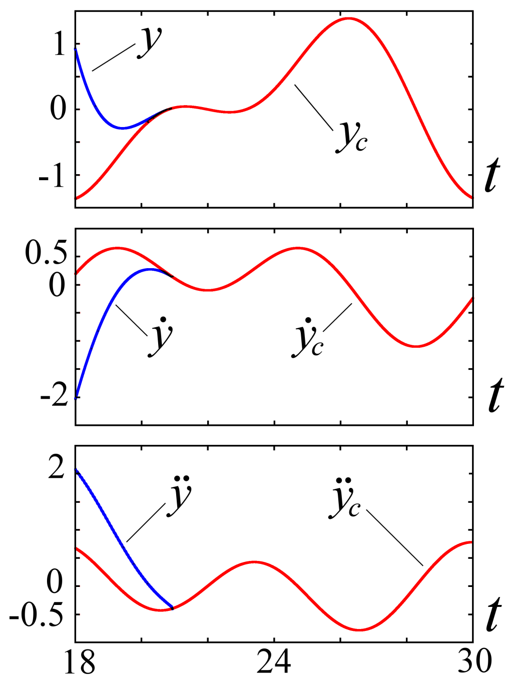

Fig. 1.15 Zoom of the tracking graphs for $y(t)$, $y_c(t)$ and their derivatives in the 3-SM Control (1.71) in the case of the 3-SM Control (1.71) with full exact measurements..

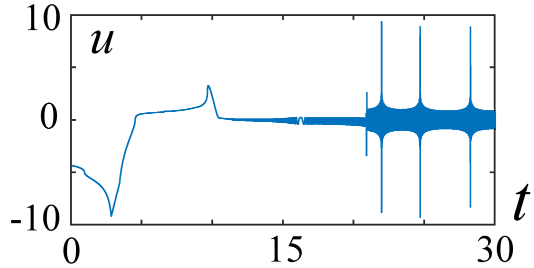

Fig. 1.16 3-SM Control (1.71) in the case of full exact measurements.

The obtained tracking accuracies are $|y - y_c| < 4 \cdot 10^{-10}$, $|\dot{y} - \dot{y}_c| < 5 \cdot 10^{-7}$ and $|\ddot{y} - \ddot{y}_c| < 5 \cdot 10^{-5}$ for $t > 25$.

Now consider the case when only the tracking error σ_y is available, and an observer/differentiator is to provide the estimations of $\vec{\sigma}_{y2}$. The differentiator outputs z_i are substituted for $\sigma_y^{(i)}$, $i = 0, 1, 2$, in the controller (1.71).

The hybrid filtering differentiator (1.34), (1.35) is chosen with $L = 100$, $M = 0.5$, $n_d = 2$, $n_f = 7$, $z(0) = (1000, -1000, 1000)$. We intentionally choose large initial observer values to demonstrate its fast convergence. The parameters λ_i, $i = 0, ..., 9$, are taken from (1.37). The differentiator discrete version (1.45), (1.46) is employed.

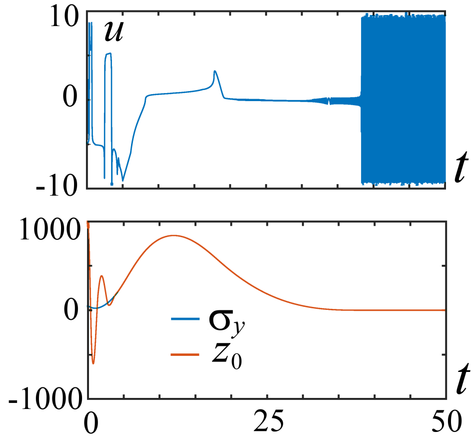

Fig. 1.17 3-SM output-feedback control in the absence of noises. Control signal and convergence of the differentiator output z_0 to the tracking error σ_y.

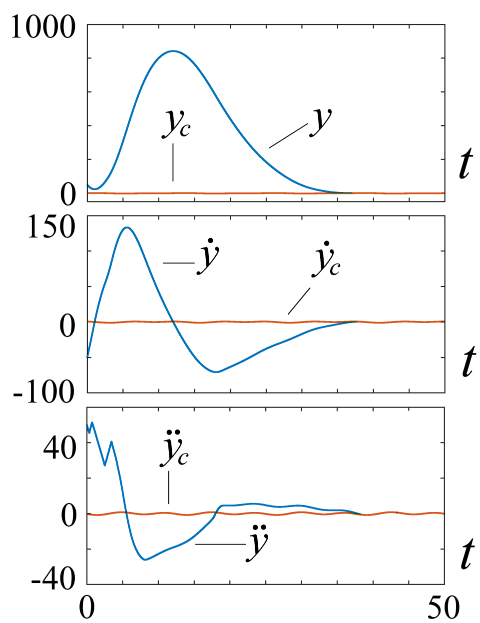

Fig. 1.18 3-SM output feedback tracking performance in the absence of noises

The performance of the output-feedback 3-SM control in the absence of noises is demonstrated in Figs. 1.17, 1.18. The resulting accuracy is $|y - y_c| < 5 \cdot 10^{-10}$, $|\dot{y} - \dot{y}_c| < 2 \cdot 10^{-6}$ and $|\ddot{y} - \ddot{y}_c| < 6 \cdot 10^{-3}$ for $t > 40$.

1.9.2.2 Output-feedback 3-SM control in the presence of noises

Let now $\sigma_y = y - y_c$ be measured with the noise

$$\begin{aligned}
&\eta(t) = \eta_1(t) + \eta_2(t) + \eta_3(t), \\
&\eta_1(t) \in \mathcal{N}(0, 0.5^2), \\
&\eta_2(t) = 10^8 \sin(5 \cdot 10^8 t), \\
&\eta_3(t) = 0.2 \cdot \sin(500000t) \cdot |\cos(500000t)|^{-0.5},
\end{aligned} \tag{1.72}$$

where $\eta_1(t)$ is a Gaussian noise of the standard deviation 0.5, $\eta_2(t)$ is a harmonic noise of extremely high magnitude and frequency, and $\eta_3(t)$ is an unbounded noise (Fig. 1.19, Example 3).

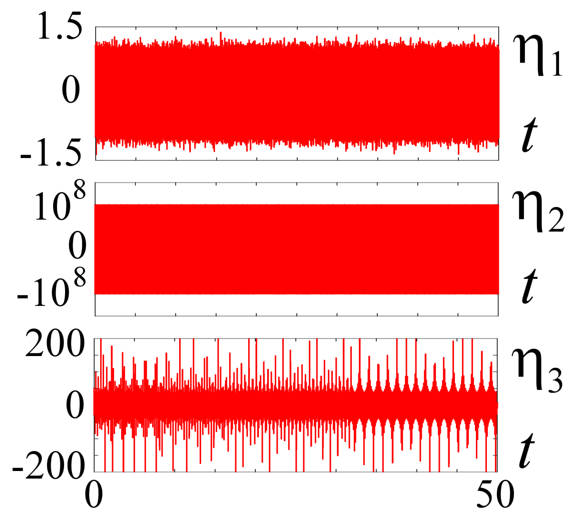

Fig. 1.19 Noises (1.72): the Gaussian noise η_1, the harmonic noise η_2, the unbounded noise η_3.

We preserve the same controller, differentiator, initial values and the sampling interval.

Note that not only the noise magnitude, but also its frequency are challenging for the differentiator. Indeed, the sampling frequency is very low compared with the frequencies of both η_2 and η_3. Under the considered sampling with interval $\tau = 10^{-6}$ both signals can be considered as discrete random signals of a not clear distribution. The numeric evaluation of the integrals is not valid, since the number of the integration points per period is less than 0.1 in the first case and less than 3 in the second.

In particular, the peaks appearing in the graph of η_3 (Fig. 1.19) are caused by some digital resonance due to the finite number of the meaningful computer number digits. Note that the differentiator indeed diverges for the harmonic-signal frequency exceeding 10^{10}.

Performance of the system in the presence of the combined noise $\eta(t)$ is demonstrated in the Fig. 1.20. The tracking accuracy is $(|\sigma_y|, |\dot{\sigma}_y|, |\ddot{\sigma}_y|) \leq (0.15, 1, 6.5)$ for $t > 45$.

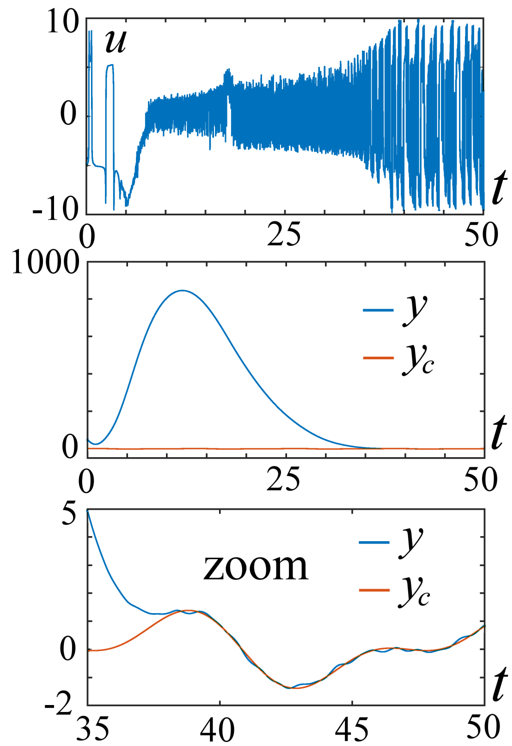

Fig. 1.20 Output-feedback 3-SM control (1.71) under the noise measurements. Control and convergence of $y(t)$ to $y_c(t)$.

1.9.3 Output-feedback robot SMC

Consider the academic example of a 1-link robot with a joint elasticity, inspired by [40] (Fig. 1.21),

$$\begin{aligned} J_1\ddot{q}_1 &= u + K(t)(q_2 - q_1) - F_1\dot{q}_1; \\ J_2\ddot{q}_2 &= -K(t)(q_2 - q_1) - F_2\dot{q}_2 - mg_n d\cos(q_2). \end{aligned} \tag{1.73}$$

Here q_1 and q_2 are the angular positions; J_1 and F_1 represent inertia and viscous constants of the actuator, $K(t)$ is the elasticity of the spring in an uncertain way depending on the environment conditions. Control u is the torque produced at the actuator axis. Similarly J_2 and F_2 are the corresponding constants of the link; m and d represent the mass and the distance to the gravity center of the link, $g_n = 9.81$ is the free-fall acceleration.

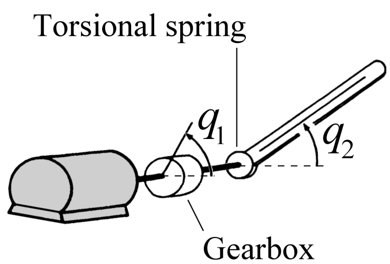

Fig. 1.21 A one-link robot.

The system would be feedback-linearizable, if $K(t)$ were a known constant. Let $J_1 = 1, F_1 = F_2 = 1, J_2 = md^2 = 1, m = 0.25, d = 2, g_n = 9.81$. The "unknown" function $K(t)$ and the signal $q_{2c}(t)$ to be tracked are chosen as $K(t) = 5 + \sin t$ and $q_{2c}(t) = \cos(0.5t) + 0.6\sin t$. The tracking error is defined as $\sigma = q_2 - q_{2c}$.

The system relative degree is 4, since $q_2^{(4)} = ... + K/(J_1J_2)u$. Correspondingly a 4-SMC of the form (1.66) is applied.

1.9.3.1 Robot output-feedback 4-SM control

Obviously system (1.73) satisfies a DI of the form (1.13) only locally. Therefore, the developed SMC is also only locally effective. In order to start the control one needs some initial values for the differentiator. Once more we choose large initial values of the differentiator which naturally correspond to an attempt to algebraically evaluate the initial tracking-error derivatives in the presence of large noises.

Apply the hybrid filtering differentiator (1.45), (1.46) with $n_d = 3$, $n_f = 7$, $L = 150, M = 0.5, z(0) = (10000, -12000, 20000, -10000)$. Note that $q_2^{(4)}$ grows fast with the norm of the system state of $(q_1, \dot{q}_1, q_2, \dot{q}_2)$, and the value $L = 150$ is not exaggerated.

Choose the system initial values $(q_1, \dot{q}_1, q_2, \dot{q}_2) = (1, -1, 1, -1)$. Let the sampling step be $\tau = 10^{-6}$. Apply control (1.66) with $\alpha = 10$ and z_i substituted for

$\sigma^{(i)}$, $i = 0, 1, 2, 3$. In order to feed the control with reasonably accurate derivative estimations, the control is only applied at $t = 10$ providing the time for the observer convergence.

Performance of the system in the absence of noises is presented in Figs. 1.22, 1.23. The system converges to the region

$$(|\sigma|, |\dot{\sigma}|, |\ddot{\sigma}|, |\dddot{\sigma}|) \leq (1.2 \cdot 10^{-6}, 5.3 \cdot 10^{-7}, 3.7 \cdot 10^{-5}, 0.06).$$

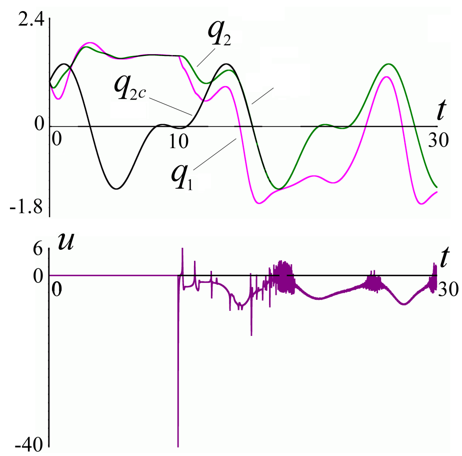

Fig. 1.22 Robot 4-SMC, hybrid differentiator in the feedback: tracking performance and control in the absence of noise. Control is applied from $t = 10$.

Let now σ be measured with the noise $\eta = 10^5 \cos(10^7 t)$ (Fig. 1.24). Once more note that the noise frequency is way too high for the sampling/integration interval $\tau = 10^{-6}$. The corresponding performance of the output-feedback controller is shown in Fig. 1.25. The tracking accuracy is

$$(|\sigma|, |\dot{\sigma}|, |\ddot{\sigma}|, |\dddot{\sigma}|) \leq (1.9 \cdot 10^{-2}, 0.026, 0.18, 4.5).$$

Let now check the performance of the homogeneous filtering differentiator with exactly the same parameters $L = 150, n_d = 3, n_f = 7$, but $M = 0$, in the absence of noises. Both differentiators are applied in the same feedback and all the parameters, initial values, etc. are the same as above. The only difference is in the parameter M. The results are presented in Fig. 1.26.

While the filtering differentiator is very stable and converges to the exact values of $\vec{\sigma}_3$ in FT, the convergence time is so long here that its application is practically impossible.

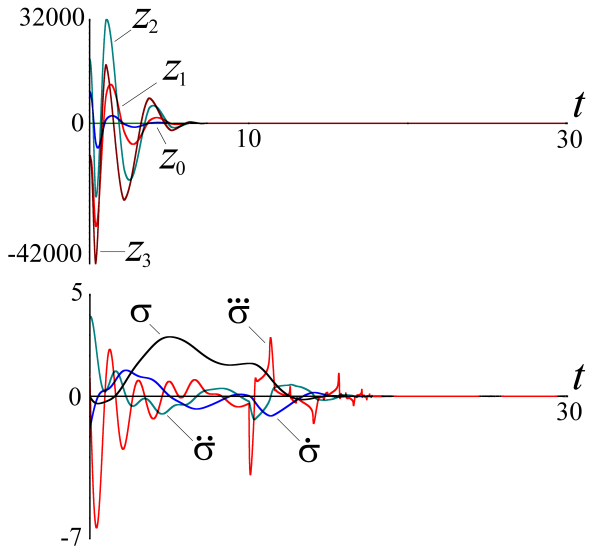

Fig. 1.23 Robot 4-SMC, hybrid differentiator in the feedback in the absence of noises. Below: convergence of the tracking errors $\sigma, \dot{\sigma}, \ddot{\sigma}, \dddot{\sigma}$ to zero; above: convergence of the differentiator outputs z_i to σ^i, $i = 0, 1, 2, 3$. Control is applied from $t = 10$ in order to provide some time for the differentiator convergence.

Fig. 1.24 Robot 4-SMC, the noise $\eta = 10^5 \cos(10^7 t)$ of the sampled tracking error $\sigma = q_2 - q_{2c}$.

1.10 Conclusion

New methodology of homogeneous SM control design and homogeneous/bihomogeneous SM-based observation are presented. Extensive numeric experiments demonstrate the effectiveness of the technique in the presence of very large and even unbounded sampling noises.

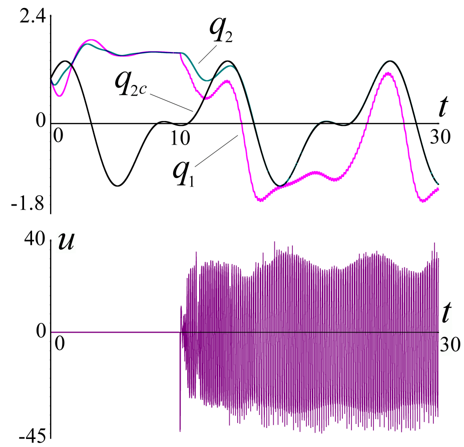

Fig. 1.25 Robot 4-SMC, hybrid differentiator in the feedback. Performance in the presence of the noise $\eta = 10^5 \cos(10^7 t)$. Above: the tracking of q_{2c} by the angle q_2 and the graph of the angle q_1. Below: the control is applied from $t = 10$.

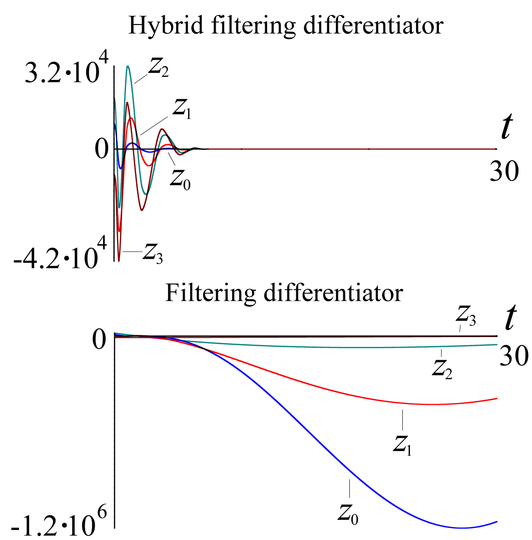

Fig. 1.26 Robot 4-SMC, with a differentiator in the feedback. Comparison in the absence of noises for the same initial values $z(0) = (10000, -12000, 20000, -10000)$. Above: Convergence of the hybrid differentiator ($M = 0.5$). Below: practical divergence of the filtering differentiator.

References

1. V. Andrieu, L. Praly, and A. Astolfi. Homogeneous approximation, recursive observer design, and output feedback. *SIAM Journal on Control and Optimization*, 47(4):1814–1850, 2008.
2. M.T. Angulo, L. Fridman, and J.A. Moreno. Output-feedback finite-time stabilization of disturbed feedback linearizable nonlinear systems. *Automatica*, 49(9):2767–2773, 2013.
3. M.T. Angulo, J.A. Moreno, and L.M. Fridman. Robust exact uniformly convergent arbitrary order differentiator. *Automatica*, 49(8):2489–2495, 2013.
4. W.A. Apaza-Perez, L. Fridman, and J.A. Moreno. Higher order sliding-mode observers with scaled dissipative stabilisers. *International Journal of Control*, 91(11):2511–2523, 2018.
5. A.N. Atassi and H.K. Khalil. Separation results for the stabilization of nonlinear systems using different high-gain observer designs. *Systems & Control Letters*, 39(3):183–191, 2000.
6. A. Bacciotti and L. Rosier. *Liapunov Functions and Stability in Control Theory*. Springer Verlag, London, 2005.
7. J.-P. Barbot, A. Levant, M. Livne, and D. Lunz. Discrete differentiators based on sliding modes. *Automatica*, 112; DOI: 10.1016/j.automatica.2019.108633:available online, 2020.
8. J.-P. Barbot, H. Saadaoui, M. Djemai, and N. Manamanni. Nonlinear observer for autonomous switching systems with jumps. *Nonlinear Analysis: Hybrid Systems*, 1(4):537—-547, 2007.
9. G. Bartolini. Chattering phenomena in discontinuous control systems. *International Journal of Systems Science*, 20:2471–2481, 1989.
10. G. Bartolini, A. Ferrara, and E. Usai. Chattering avoidance by second-order sliding mode control. *IEEE Transactions on Automatic Control*, 43(2):241–246, 1998.
11. G. Bartolini, A. Pisano, E. Punta, and E. Usai. A survey of applications of second-order sliding mode control to mechanical systems. *International Journal of Control*, 76(9/10):875–892, 2003.
12. E. Bernuau, D. Efimov, W. Perruquetti, and A. Polyakov. On homogeneity and its application in sliding mode control. *Journal of the Franklin Institute*, 351(4):1866–1901, 2014.
13. E. Bernuau, A. Polyakov, D. Efimov, and W. Perruquetti. Verification of ISS, iISS and IOSS properties applying weighted homogeneity. *Systems & Control Letters*, 62(12):1159–1167, 2013.
14. S.P. Bhat and D.S. Bernstein. Geometric homogeneity with applications to finite-time stability. *Mathematics of Control, Signals and Systems*, 17(2):101–127, 2007.
15. I. Boiko, L. Fridman, A. Pisano, and E. Usai. Analysis of chattering in systems with second-order sliding modes. *IEEE transactions on Automatic control*, 52(11):2085–2102, 2007.
16. A. Chalanga, S. Kamal, L.M. Fridman, B. Bandyopadhyay, and J.A. Moreno. Implementation of super-twisting control: Super-twisting and higher order sliding-mode observer-based approaches. *IEEE Transactions on Industrial Electronics*, 63(6):3677–3685, 2016.
17. F.H. Clarke, Y.S. Ledayev, and R.J. Stern. Asymptotic stability and smooth Lyapunov functions. *Journal of Differential Equations*, 149(1):69–114, 1998.
18. E. Cruz-Zavala and J.A. Moreno. Lyapunov approach to higher-order sliding mode design. In *Recent Trends in Sliding Mode Control*, pages 3–28. Institution of Engineering and Technology IET, London, 2016.
19. E. Cruz-Zavala and J.A. Moreno. Homogeneous high order sliding mode design: A Lyapunov approach. *Automatica*, 80:232–238, 2017.
20. E. Cruz-Zavala and J.A. Moreno. Levant's arbitrary order exact differentiator: a Lyapunov approach. *IEEE Transactions on Automatic Control*, 64(7):3034–39, 2019.
21. E. Cruz-Zavala, J.A. Moreno, and L. Fridman. Uniform robust exact differentiator. *IEEE Transactions on Automatic Control*, 56(11):2727–2733, 2012.
22. E. Cruz-Zavala, J.A. Moreno, and L. Fridman. Uniform sliding mode controllers and uniform sliding surfaces. *IMA Journal of Mathematical Control and Information*, 29(4):491–505, 2012.
23. M. Defoort, T. Floquet, A. Kokosy, and W. Perruquetti. A novel higher order sliding mode control scheme. *Systems & Control Letters*, 58(2):102–108, 2009.
24. S.H. Ding, A. Levant, and S.H. Li. Simple homogeneous sliding-mode controller. *Automatica*, 67(5):22–32, 2016.

25. F. Dinuzzo and A. Ferrara. Higher order sliding mode controllers with optimal reaching. *IEEE Transactions on Automatic Control*, 54(9):2126–2136, 2009.
26. Y. Dvir, D. Efimov, A. Levant, A. Polyakov, and W. Perruquetti. Acceleration of finite-time stable homogeneous systems. *International Journal of Robust and Nonlinear Control*, 28(5):1757–1777, 2018.
27. C. Edwards and S.K. Spurgeon. *Sliding Mode Control: Theory And Applications*. Taylor & Francis, London, 1998.
28. D. Efimov, A. Levant, A. Polyakov, and W. Perruquetti. Discretization of asymptotically stable homogeneous systems by explicit and implicit Euler methods. In *55th IEEE Conference on Decision and Control, CDC'2016, Las-Vegas, December 12-14*, 2016.
29. D.V. Efimov and L. Fridman. A hybrid robust non-homogeneous finite-time differentiator. *IEEE Transactions on Automatic Control*, 56(5):1213–1219, 2011.
30. Y. Feng, X. Yu, and Z. Man. Non-singular terminal sliding mode control of rigid manipulators. *Automatica*, 38(12):2159–2167, 2002.
31. A.F. Filippov. *Differential Equations with Discontinuous Right-Hand Sides*. Kluwer Academic Publishers, Dordrecht, 1988.
32. T. Floquet and J.-P. Barbot. Super twisting algorithm-based step-by-step sliding mode observers for nonlinear systems with unknown inputs. *International Journal of Systems Science*, 38(10):803–815, 2007.
33. T. Floquet, J.P. Barbot, and W. Perruquetti. Higher-order sliding mode stabilization for a class of nonholonomic perturbed systems. *Automatica*, 39(6):1077–1083, 2003.
34. L. Fridman. Chattering analysis in sliding mode systems with inertial sensors. *International Journal of Control*, 76(9/10):906–912, 2003.
35. L. Fridman, J.A. Moreno, B. Bandyopadhyay, S. Kamal, and A. Chalanga. Continuous nested algorithms: The fifth generation of sliding mode controllers. In *Recent Advances in Sliding Modes: From Control to Intelligent Mechatronics*, pages 5–35. Springer International Publishing, 2015.
36. Z. Galias and X. Yu. Euler's discretization of single input sliding-mode control systems. *IEEE Transactions on Automatic Control*, 52(9):1726–1730, 2007.
37. A. Hanan, A. Jbara, and A. Levant. Homogeneous output-feedback control. In *Proc. of the 21th IFAC World Congress, Berlin, July 13-17, Germany*, 2020.
38. A. Hanan, A. Jbara, and A. Levant. New homogeneous controllers and differentiators. In *Variable-Structure Systems and Sliding-Mode Control*, pages 3–28. Springer, 2020.
39. M. Harmouche, S. Laghrouche, Y. Chitour, and M. Hamerlain. Stabilisation of perturbed chains of integrators using Lyapunov-based homogeneous controllers. *International Journal of Control*, 90(12):2631–2640, 2017.
40. A. Isidori. *Nonlinear control systems I*. Springer Verlag, New York, 1995.
41. M. Kawski. Homogeneous stabilizing feedback laws. *Control Theory and Advanced Technology*, 6:497–516, 1990.
42. S. Koch, M. Reichhartinger, M. Horn, and L. Fridman. Discrete-time implementation of homogeneous differentiators. *IEEE Transactions on Automatic Control*, 65(2):757–762, 2020.
43. S. Laghrouche, F. Plestan, and A. Glumineau. Higher order sliding mode control based on integral sliding mode. *Automatica*, 43(3):531–537, 2007.
44. A. Levant. Sliding order and sliding accuracy in sliding mode control. *International J. Control*, 58(6):1247–1263, 1993.
45. A. Levant. Robust exact differentiation via sliding mode technique. *Automatica*, 34(3):379–384, 1998.
46. A. Levant. Higher order sliding modes, differentiation and output-feedback control. *International J. Control*, 76(9/10):924–941, 2003.
47. A. Levant. Homogeneity approach to high-order sliding mode design. *Automatica*, 41(5):823–830, 2005.
48. A. Levant. Quasi-continuous high-order sliding-mode controllers. *IEEE Trans. Aut. Control*, 50(11):1812–1816, 2005.
49. A. Levant. Chattering analysis. *IEEE Transactions on Automatic Control*, 55(6):1380–1389, 2010.

50. A. Levant. On fixed and finite time stability in sliding mode control. In *Proc. of the 52 IEEE Conference on Decision and Control, Florence, Italy, December 10-13, 2013*, 2013.
51. A. Levant. Non-Lyapunov homogeneous SISO control design. In *56th Annual IEEE Conference on Decision and Control (CDC), Melbourne, VIC, Australia, Dec. 12-15 , 2017*, pages 6652–6657, 2017.
52. A. Levant. Filtering differentiators and observers. In *15th International Workshop on Variable Structure Systems (VSS), Graz, Austria, July 9-11, 2018*, pages 174–179, 2018.
53. A. Levant. Sliding Mode Control: Finite-Time Observation and Regulation. In *Baillieul J., Samad T. (eds), Encyclopedia of Systems and Control*. Springer, London, 2021. URL: https://doi.org/10.1007/978-1-4471-5102-9_100069-1.
54. A. Levant, D. Efimov, A. Polyakov, and W. Perruquetti. Stability and robustness of homogeneous differential inclusions. In *Proc. of the 55th IEEE Conference on Decision and Control, Las-Vegas, December 12-14, 2016*, 2016.
55. A. Levant and M. Livne. Exact differentiation of signals with unbounded higher derivatives. *IEEE Transactions on Automatic Control*, 57(4):1076–1080, 2012.
56. A. Levant and M. Livne. Uncertain disturbances' attenuation by homogeneous MIMO sliding mode control and its discretization. *IET Control Theory & Applications*, 9(4):515–525, 2015.
57. A. Levant and M. Livne. Weighted homogeneity and robustness of sliding mode control. *Automatica*, 72(10):186–193, 2016.
58. A. Levant and M. Livne. Globally convergent differentiators with variable gains. *International Journal of Control*, 91(9):1994–2008, 2018.
59. A. Levant and M. Livne. Robust exact filtering differentiators. *European Journal of Control*, 55(9):33–44, 2020.
60. A. Levant, M. Livne, and X. Yu. Sliding-mode-based differentiation and its application. *IFAC-PapersOnLine*, 50(1):1699–1704, 2017.
61. A. Levant and X. Yu. Sliding-mode-based differentiation and filtering. *IEEE Transactions on Automatic Control*, 63(9):3061–3067, 2018.
62. M. Livne and A. Levant. Proper discretization of homogeneous differentiators. *Automatica*, 50:2007–2014, 2014.
63. Z. Man, A.P. Paplinski, and H. Wu. A robust MIMO terminal sliding mode control scheme for rigid robotic manipulators. *IEEE Transactions on Automatic Control*, 39(12):2464–2469, 1994.
64. J.A. Moreno. Levant's arbitrary order differentiator with varying gain. In *Proc. of the 20th IFAC World Congress, Toulouse, July 9-14, France, 2017*, 2017.
65. J.A. Moreno and M. Osorio. Strict Lyapunov functions for the super-twisting algorithm. *IEEE Transactions on Automatic Control*, 57(4):1035–1040, 2012.
66. W. Perruquetti, T. Floquet, and E. Moulay. Finite-time observers: application to secure communication. *Automatic Control, IEEE Transactions on*, 53(1):356–360, 2008.
67. A. Pisano and E. Usai. Sliding mode control: A survey with applications in math. *Mathematics and Computers in Simulation*, 81(5):954–979, 2011.
68. F. Plestan, A. Glumineau, and S. Laghrouche. A new algorithm for high-order sliding mode control. *International Journal of Robust and Nonlinear Control*, 18(4/5):441–453, 2008.
69. A. Polyakov. Sliding mode control design using canonical homogeneous norm. *International Journal of Robust and Nonlinear Control*, 29(3):682–701, 2019.
70. A. Polyakov, D. Efimov, and W. Perruquetti. Finite-time and fixed-time stabilization: Implicit Lyapunov function approach. *Automatica*, 51(1):332–340, 2015.
71. A. Polyakov, D. Efimov, and W. Perruquetti. Robust stabilization of MIMO systems in finite/fixed time. *International Journal of Robust and Nonlinear Control*, 26(1):69–90, 2016.
72. A. Polyakov and L. Fridman. Stability notions and Lyapunov functions for sliding mode control systems. *Journal of The Franklin Institute*, 351(4):1831–1865, 2014.
73. M. Reichhartinger and S. Spurgeon. An arbitrary-order differentiator design paradigm with adaptive gains. *International Journal of Control*, 91(9):2028–2042, 2018.
74. T. Sanchez, J.A. Moreno, and L.M. Fridman. Output feedback continuous twisting algorithm. *Automatica*, 96:298–305, 2018.

75. Y. Shtessel, C. Edwards, L. Fridman, and A. Levant. *Sliding mode control and observation*. Birkhauser, Basel, 2014.
76. Y.B. Shtessel and I.A. Shkolnikov. Aeronautical and space vehicle control in dynamic sliding manifolds. *International Journal of Control*, 76(9/10):1000–1017, 2003.
77. V.I. Utkin. *Sliding Modes in Control and Optimization*. Springer Verlag, Berlin, Germany, 1992.
78. V.I. Utkin. Sliding mode control design principles and applications to electric drives. *IEEE Transactions on Industrial Electronics*, 40(1):23–36, 1993.